

UNCLASSIFIED

AD **407 957**

DEFENSE DOCUMENTATION CENTER

FOR

SCIENTIFIC AND TECHNICAL INFORMATION

CAMERON STATION, ALEXANDRIA, VIRGINIA



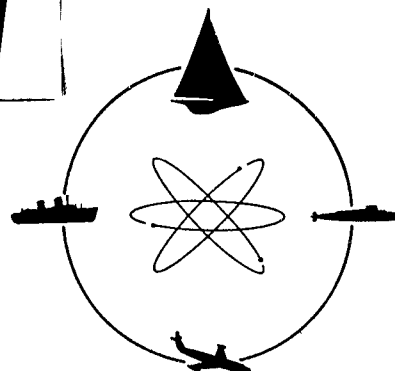
UNCLASSIFIED

NOTICE: When government or other drawings, specifications or other data are used for any purpose other than in connection with a definitely related government procurement operation, the U. S. Government thereby incurs no responsibility, nor any obligation whatsoever; and the fact that the Government may have formulated, furnished, or in any way supplied the said drawings, specifications, or other data is not to be regarded by implication or otherwise as in any manner licensing the holder or any other person or corporation, or conveying any rights or permission to manufacture, use or sell any patented invention that may in any way be related thereto.

63-4-1

R-940

407 957



DAVIDSON LABORATORY



STEVENSON
OF TECHNOLOGY

CASTLE POINT STATION
HOBOKEN, NEW JERSEY

Report 940

JUN 13 1963

TISIA A

THREE-DIMENSIONAL APPROACH
TO THE GUST PROBLEM
FOR A SCREW PROPELLER

by

J. Shioiri and S. Tsakonas

March 1963

R-940

DAVIDSON LABORATORY
REPORT 940

March 1963

THREE-DIMENSIONAL APPROACH TO THE
GUST PROBLEM FOR A SCREW PROPELLER

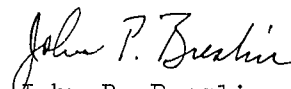
by

J. Shioiri and S. Tsakonas

Contract Nonr 263(38) and Nobs 68349
Bureau of Ships Fundamental
Hydromechanics Research Program
S-R 009 01 01
Administered by David Taylor Model Basin

Reproduction in whole or in part is permitted
for any purpose of the United States Government

Approved


John P. Breslin
Director

ABSTRACT

The unsteady lifting surface approach is utilized for the marine propeller case and the corresponding surface integral equation is solved for the Weissinger mathematical model. The applicability of the Weissinger method to the nonstationary flow case is studied. The kernel function is expressed in closed forms after some mathematical simplification. From numerical calculations of propeller loading which are restricted to a four-bladed propeller of sector type blade form with different blade-area ratios and various pitch-diameter ratios, conclusions are drawn as to three-dimensional effects as well as to the dependence of propeller loading on the important parameters, as the blade-area and pitch-diameter ratios.

TABLE OF CONTENTS

	<u>Page</u>
Abstract	iii
Introduction	1
Formulation of Problem	2
Solution by the Weissinger Approximation	5
Application of the Weissinger Method and Solving Procedure	5
Simplification of the Kernel	7
Evaluation of the Kernel	10
Numerical Results and Discussion	16
Conclusions	19
Acknowledgments	19
References	20
Table	
Figures	
Appendix A	
Appendix B	
Appendix C	
Appendix D	
Appendix E	

INTRODUCTION

The ship hull induces a disturbance flow upon the propeller plane. Although, in general, this flow is time-independent, its distribution on the propeller plane is non-uniform, and hence the rotating blades, which cut through this disturbance, experience time-dependent gust. If this disturbance flow is expanded into angular harmonics, each component exerts a sinusoidal gust upon the blades. Using Sears' two-dimensional response function for the sinusoidal gust¹ in a stripwise manner, Breslin et al² evaluated the oscillatory thrust and torque of the propeller due to this kind of disturbance. However, correlation with existing experimental results was very poor,³ and they attributed this to application of the two-dimensional method to a typically three-dimensional problem.

At this stage, it seems important to try a three-dimensional approach. The three-dimensional lifting surface integral equation for the screw propeller in a steady flow was derived by Sparenberg.⁴ A slight modification gives the equation for the non-steady state. The nature of this equation was examined by Hanaoka.⁵

Owing to the complicated form of the kernel, however, it seems difficult to treat this equation in an exact form. In this report, by adopting the Weissinger approximation, the surface integral equation is converted into a spanwise line equation. The applicability of the Weissinger method to the three-dimensional propeller problem in the steady condition has been well examined, but applicability to the non-steady problem remains to be tested. In Appendix A the two-dimensional sinusoidal gust problem is treated under the Weissinger approximation and the result is compared with Sears' exact value. The result is also applied stripwise to

the present problem and a comparison with the results of the three-dimensional Weissinger approach is shown. This comparison (both approaches are obtained under the same Weissinger approximation) will provide important knowledge on the three-dimensional effect in the non-steady state.

FORMULATION OF PROBLEM

In this section the derivation of the integral equation for the angular harmonic component of the disturbance flow is shown. Use is made of the acceleration potential method. The necessary notations concerning the coordinate system are shown in Fig. 1.

The pressure field $P_p(x, r, \phi)$ due to a unit pressure pole $l(\xi, \rho, \theta)$ is given by

$$P_p = \frac{1}{4\pi} \frac{1}{\sqrt{(x-\xi)^2 + r^2 + \rho^2 - 2r\rho \cos(\theta-\phi)}} \quad (1)$$

If the pole is pulsating in its strength with frequency ω and rotating in the negative direction of θ with angular velocity Ω ,

$$P_p = \frac{1}{4\pi} \frac{e^{i\omega t}}{\sqrt{(x-\xi)^2 + r^2 + \rho^2 - 2r\rho \cos(\theta_0 - \Omega t - \phi)}} \quad (2)$$

The linearized relation between the perturbation velocity potential $\Phi(x, r, \phi, t)$ and the corresponding pressure field $P(x, r, \phi, t)$ in the main (x -direction) uniform flow U is given by

$$U \frac{\partial \Phi}{\partial x} + \frac{\partial \Phi}{\partial t} = -\frac{1}{\mu} P \quad (3)$$

where μ is the density of the fluid. If it is assumed that $\Phi = 0$ at $x = -\infty$, the solution Φ for given P is

$$\Phi = -\frac{1}{\mu U} \int_{-\infty}^x P(\tau', r, \phi, t + \frac{\tau' - x}{U}) d\tau' \quad (4)$$

On substituting eq. 2 into eq. 4 and putting $\tau' = \tau + \xi$, the velocity potential Φ_p corresponding to P_p of eq. 2 becomes

$$\Phi_p = -\frac{e^{i\omega t}}{4\pi\mu U} \int_{-\infty}^{x-\xi} \frac{e^{\frac{i\omega}{U}(\tau-x+\xi)}}{\sqrt{\tau^2+r^2+\rho^2-2r\rho\cos[\theta_0-\Omega t-\frac{\Omega}{U}(\tau-x+\xi)-\phi]}} d\tau \quad (5)$$

When the observation point (x, r, ϕ) is rotating together with the pressure pole, putting $\phi = \phi_0 - \Omega t$,

$$\Phi_p = -\frac{e^{i\omega t}}{4\pi\mu U} \int_{-\infty}^{x-\xi} \frac{e^{\frac{i\omega}{U}(\tau-x+\xi)}}{\sqrt{\tau^2+r^2+\rho^2-2r\rho\cos[(\theta_0-\phi_0)-\frac{\Omega}{U}(\tau-x+\xi)]}} d\tau \quad (6)$$

If the pressure pole is replaced by a dipole, the corresponding velocity potential Φ_d is

$$\Phi_d = \frac{\partial}{\partial \chi} \Phi_p, \quad (7)$$

where $\frac{\partial}{\partial \chi}$ is a differential operator with respect to (ξ, ρ, θ_0) in the direction of the dipole axis. Velocity induced by this dipole is

$$W_d(x, r, \phi_0) = \frac{\partial}{\partial \chi'} \Phi_d = \frac{\partial}{\partial \chi'} \frac{\partial}{\partial \chi} \Phi_p \quad (8)$$

where $\frac{\partial}{\partial \chi'}$ is an operator with respect to (x, r, ϕ_0) in the designated direction of the velocity.

In the acceleration potential method, the lifting surface is regarded as a mono-layer of pressure dipoles, the axis of which is normal to the surface and the strength of which is proportional to the pressure jump across the surface. Therefore, it is easily seen that eq. 8 is the elementary component of the lifting surface integral equation for the simple harmonically time-dependent problem of a rotating system.

The phenomena appearing at corresponding points on all blades due to the qth harmonics of the disturbance flow are expressed in the following simple form:

$$\zeta_n = \zeta_o e^{iq[\Omega t - \bar{\theta}_n]} \quad (9)$$

where $\bar{\theta}_n = \frac{2\pi}{N}(n-1)$, n is the name of the blade $n = 1, 2, \dots, N$, and N is the total number of blades. Summing up the effect of all blades upon a particular blade ($n = 1$), and considering that the geometrical equation of the lifting surface of the screw propeller is expressed by

$$x = \frac{1}{a} \phi_o \text{ (or } \xi = \frac{1}{a} \theta_o \text{), where } a = \frac{\Omega}{U}, \quad (10)$$

leads to the integral equation for the present problem which can be written as

$$V(r) e^{iq(\Omega t - \phi_o)} = e^{iq\Omega t} \int_p \int_{\theta_o} S(\rho, \theta_o) K(r, \phi_o, \rho, \theta_o) d\theta_o d\rho \quad (11)$$

Here $S(\rho, \theta_o)$ is the lift distribution on the blade, and $K(r, \phi_o, \rho, \theta_o)$ is the kernel, which is obtained in the following form by using eqs. 6 to 10:

$$K(r, \phi_o, \rho, \theta_o) = - \frac{1}{4\pi\mu U} \sum_{n=1}^N \lim_{\delta = \frac{1}{a}(\phi_o - \theta_o) - (x - \xi) \rightarrow 0} \left[\frac{\partial}{\partial \chi} \frac{\partial}{\partial \chi'} \cdot \right. \\ \left. \int_{-\infty}^{x-\xi} \frac{e^{iq[-\bar{\theta}_n + a(\tau - x + \xi)]}}{\sqrt{\tau^2 + r^2 + \rho^2 - 2r\rho \cos[(\theta_o - \phi_o) + \bar{\theta}_n - a(\tau - x + \xi)]}} d\tau \right] \quad (12)$$

The directions of the differentiations in $\frac{\partial}{\partial \chi}$ and $\frac{\partial}{\partial \chi'}$ are perpendicular to the lifting surface, that is, from eq. 10

$$\begin{aligned}\frac{\partial}{\partial \chi'} &= \frac{r}{\sqrt{1+a^2 r^2}} \left(a \frac{\partial}{\partial x} - \frac{1}{r^2} \frac{\partial}{\partial \phi_0} \right) \\ \frac{\partial}{\partial \chi} &= \frac{\rho}{\sqrt{1+a^2 \rho^2}} \left(a \frac{\partial}{\partial \xi} - \frac{1}{\rho^2} \frac{\partial}{\partial \theta_0} \right)\end{aligned}\tag{13}$$

The limiting process

$$\lim_{a \rightarrow 0} \delta = (x - \xi) - \frac{1}{a}(\phi_0 - \theta_0) \rightarrow 0$$

is introduced in order to avoid the difficulty due to the singularity in the mathematical manipulations. Physically, it means that the manipulations are performed taking the controlling point on a surface slightly shifted from the lifting surface and that finally the former surface is brought infinitesimally close to the latter.

SOLUTION BY THE WEISSINGER APPROXIMATION

APPLICATION OF THE WEISSINGER METHOD AND SOLVING PROCEDURE

In the Weissinger method, the surface distribution of the lift is replaced by a line distribution along the 1/4-chord line, and the controlling points are taken along the 3/4-chord line. This method gives an exact lift for the two-dimensional stationary wing problem, and it is applicable also to the stationary three-dimensional wing problem under the assumption of not too low aspect ratio. In fact, in the stationary propeller problem, it has been shown that this method can describe the effect of the helical free vortex fairly well.

However, in the nonstationary case, there is another kind of free vortex which is parallel to the span (in the propeller problem the radial free vortex), and it seems not

to have been clarified how precisely the Weissinger model can obtain the effect of the latter kind of free vortex. The applicability of this method to the nonstationary problem is tested in Appendix A by treating the two-dimensional sinusoidal gust problem. The result indicates that this method can be used up to a reduced frequency of 1.3, which corresponds to blade frequency harmonics ($q = N$) in a propeller of area ratio 0.4.

This approximation is based upon the first and second terms of Birnbaum's chordwise lift distribution, and hence on the left-hand side of the integral equation the corresponding components should be picked up. In the two-dimensional stationary case, this can be done exactly by applying Glauert's lift operator,

$\int_0^\pi (1 - \cos \alpha) d\alpha$ where $x = -b \cos \alpha$, x is the chordwise coordinate and b is the semi-chord length. The same operator is tried for the two-dimensional but nonstationary case in Appendix A, and the result indicates its satisfactory application to the nonstationary case up to the reduced frequency 1.3. In the following treatment, the same procedure will be used for the nonstationary three-dimensional case under the assumption of a not too low aspect ratio.

Thus, the application of the Weissinger method converts eq. 11 (the surface integral equation) into the following line integral equation:

$$W(r) = \int_0^1 L(\rho) K(r, \rho) d\rho, \quad (14)$$

where

$$W(r) = V(r) \int_0^\pi e^{iq\bar{\theta}_b \cos \alpha} (1 - \cos \alpha) d\alpha, \quad (15)$$

$L(\rho)$ is spanwise line distribution of lift,

$$K(r, \rho) = [K(r, \phi_0, \rho, \theta_0)]_{\phi_0 - \theta_0 = \bar{\theta}_b}, \quad (16)$$

and

$\bar{\theta}_b$ is semi-chord length.

The integral equation (eq. 14) can be treated in the following way. By dividing the span into intervals of equal length 2ℓ , and regarding the lift distribution on each fraction as uniform, eq. 16 can be written in the form of a set of simultaneous linear algebraic equations

$$\begin{bmatrix} W_p \end{bmatrix} = \begin{bmatrix} K_{pq} \end{bmatrix} \begin{bmatrix} L_q \end{bmatrix}. \quad (17)$$

The element of the kernel matrix is given by

$$K_{pq} = \int_{r_q - \ell}^{r_q + \ell} K(r_p, \rho) d\rho. \quad (18)$$

The singularity of eq. 12 is involved in the element K_{pp} , but that singularity is integrable in the ρ integration. Thus, the kernel matrix elements are free from singular behavior, and the spanwise lift distribution L_q for given W_p , and, in addition, the inverse matrix of $\begin{bmatrix} K_{pq} \end{bmatrix}$, can be obtained without any difficulty. In the nonstationary problem, all the elements in eq. 17 are complex numbers. Hence, if the span is divided into P parts, the kernel matrix is of the order $2P \times 2P$, but a conventional digital computer can easily give the required results.

SIMPLIFICATION OF THE KERNEL

By putting $y = -a(\tau - x + \xi)$, interchanging the order of the integral sign and differential operation in eq. 12 becomes possible. The term within the brackets of eq. 12, designated now by H , becomes on substituting eq. 13,

$$H = -\frac{1}{a} \int_0^{\infty} e^{-iq(\bar{\theta}_n + y)} \frac{r}{\sqrt{1+a^2 r^2}} \left(a \frac{\partial}{\partial x} - \frac{1}{r^2} \frac{\partial}{\partial \phi_0} \right) \frac{\rho}{\sqrt{1+a^2 \rho^2}} \left(a \frac{\partial}{\partial \xi} - \frac{1}{\rho^2} \frac{\partial}{\partial \theta_0} \right) \frac{1}{\sqrt{\left[\frac{1}{a} y - (x - \xi) \right]^2 + r^2 + \rho^2 - 2r\rho \cos \left[(\theta_0 - \phi_0) + \bar{\theta}_n + y \right]}} dy \quad (19)$$

Further, if

$$\frac{1}{a} y - (x - \xi) = X \text{ and } \bar{\theta}_n + (\theta_0 - \phi_0) + y = \theta, \quad (20)$$

$$H = -\frac{1}{a} \int_0^{\infty} e^{-iq(\bar{\theta}_n + y)} \left[\frac{r}{\sqrt{1+a^2 r^2}} \left(a \frac{\partial}{\partial x} - \frac{1}{r^2} \frac{\partial}{\partial \theta} \right) \frac{\rho}{\sqrt{1+a^2 \rho^2}} \left(a \frac{\partial}{\partial x} - \frac{1}{\rho^2} \frac{\partial}{\partial \theta} \right) \frac{1}{\sqrt{X^2 + r^2 + \rho^2 - 2r\rho \cos \theta}} \right]_{\theta = \bar{\theta}_n + (\theta_0 - \phi_0) + y}^{X = \frac{1}{a} y - (x - \xi)} dy \quad (21)$$

Changing the integral variable from y to θ

$$H = -\frac{1}{a} \int_{\bar{\theta}_n + (\theta_0 - \phi_0)}^{\infty} e^{-iq[\theta - (\theta_0 - \phi_0)]} \left[\frac{-r}{\sqrt{1+a^2 r^2}} \left(a \frac{\partial}{\partial x} - \frac{1}{r^2} \frac{\partial}{\partial \theta} \right) \frac{\rho}{\sqrt{1+a^2 \rho^2}} \left(a \frac{\partial}{\partial x} - \frac{1}{\rho^2} \frac{\partial}{\partial \theta} \right) \frac{1}{\sqrt{X^2 + r^2 + \rho^2 - 2r\rho \cos \theta}} \right]_{X = \frac{1}{a} \theta - \frac{1}{a} \bar{\theta}_n + \delta}^{d\theta} \quad (22)$$

where, $\delta = \frac{1}{a} (\phi_0 - \theta_0) - (x - \xi)$

Here, under the assumption that the pitch of the propeller is low--i.e., a is large--the following two approximations are introduced:

$$1) \frac{-r}{\sqrt{1+a^2 r^2}} \left(a \frac{\partial}{\partial x} - \frac{1}{r^2} \frac{\partial}{\partial \theta} \right) \rightarrow \frac{-\partial}{\partial x}$$

$$\frac{\rho}{\sqrt{1+a^2 \rho^2}} \left(a \frac{\partial}{\partial x} - \frac{1}{\rho^2} \frac{\partial}{\partial \theta} \right) \rightarrow \frac{\partial}{\partial x}$$
(23)

- 2) the change shown in Fig. 2 of the integral path in eq. 22 from the original one expressed by light solid lines to the heavy solid lines.

These two approximations give K , eq. 12, in the following form:

$$K = \frac{1}{4\pi\mu Ua} e^{-iq\bar{\theta}_b} [K_1 + K_2],$$

where,

$$K_1 = \sum_{n=1}^N \lim_{\delta \rightarrow 0} \int_{\bar{\theta}_n - (\phi_o - \theta_o)}^{\bar{\theta}_n + (\bar{\theta}_o/2)} \left[- \frac{\partial^2}{\partial x^2} \frac{e^{-iq\theta}}{\sqrt{x^2 + r^2 + \rho^2 - 2r\rho \cos \theta}} \right]_{x=\delta} d\theta$$

$$K_2 = \lim_{\delta \rightarrow 0} \sum_{m=1}^{\infty} \int_0^{2\pi} \left[- \frac{\partial^2}{\partial x^2} \frac{e^{-iq\theta}}{\sqrt{x^2 + r^2 + \rho^2 - 2r\rho \cos \theta}} \right]_{x=m\frac{1}{a}\bar{\theta}_o + \delta} d\theta$$
(24)

$$\bar{\theta}_o = \frac{2\pi}{N}$$

and $(\phi_o - \theta_o) = \bar{\theta}_b$ in the Weissinger approximation.

The approximations 1) and 2) are rather rough ones if they are adopted separately, but their combined use is justified by a clear geometrical meaning as well as good numerical results. This point is discussed in Appendix B.

It is also worthy of notice that K_1 depends upon $\bar{\theta}_b$, the semi-chord length, but is independent of a , the inverse of pitch. On the other hand, K_2 depends upon the pitch but is independent of the chord length. This fact is a great convenience for the numerical calculations.

EVALUATION OF THE KERNEL

K₁ . When $\rho \neq r$, the limiting process $\delta \rightarrow 0$ can be taken before the integration, then

$$K_1 = \sum_{n=1}^N \int_{\bar{\theta}_n - \bar{\theta}_b}^{\bar{\theta}_n + (\bar{\theta}_o/2)} \frac{e^{-iq\theta}}{(\sqrt{r^2 + \rho^2 - 2r\rho \cos \theta})^3} d\theta \quad (25)$$

Further,

$$\begin{aligned} & \int_{\bar{\theta}_n - \bar{\theta}_b}^{\bar{\theta}_n + \bar{\theta}_o/2} \frac{e^{-iq\theta}}{\sqrt{r^2 + \rho^2 - 2r\rho \cos \theta}^3} d\theta \\ &= (-1)^{q+1} \frac{2}{(r+\rho)^3} \int_{-1/2(\pi + \bar{\theta}_n - \bar{\theta}_b)}^{-1/2(\pi + \bar{\theta}_n - \bar{\theta}_o/2)} \frac{e^{i2q\psi}}{\sqrt{1 - k^2 \sin^2 \psi}^3} d\psi \end{aligned} \quad (26)$$

where,

$$\psi = -\frac{1}{2}(\pi + \theta) \text{ and } k^2 = \frac{4r\rho}{(r+\rho)^2} \quad (27)$$

As is shown in Appendix C, the integral

$$I_q = \int_{\psi_\ell}^{\psi_u} \frac{e^{i2q\psi}}{\sqrt{1 - k^2 \sin^2 \psi}^3} d\psi \quad (28)$$

can be evaluated by the following recurrence formula:

$$I_{n+1} = \frac{4n}{2n-1} \left(1 - \frac{2}{k^2}\right) I_n - \left(\frac{2n+1}{2n-1}\right) I_{n-1}$$

$$-i \frac{2}{2n-1} \frac{2}{k^2} \frac{e^{i2n\psi}}{\sqrt{1 - k^2 \sin^2 \psi}} \Big|_{\psi_\ell}^{\psi_u},$$

and

$$I_0 = \frac{1}{1-k^2} \left[E(k, \psi) - \frac{k^2}{2} \frac{\sin^2 \psi}{\sqrt{1-k^2 \sin^2 \psi}} \right] \Big|_{\psi_\ell}^{\psi_u}$$

$$I_1 = \left(1 - \frac{2}{k^2}\right) I_0 + \frac{2}{k^2} F(k, \psi) \Big|_{\psi_\ell}^{\psi_u} + i \frac{2}{k^2} \frac{1}{\sqrt{1-k^2 \sin^2 \psi}} \Big|_{\psi_\ell}^{\psi_u} \quad (29)$$

where $F(k, \psi)$ and $E(k, \psi)$ are elliptic integrals of the first and second kind, respectively. In the case of $p \neq q$, the integration with respect to ρ in eq. 18 can be evaluated by conventional numerical methods or by taking some conventional mean value.

In the narrow band expressed by $|\rho - r_p| < r_p$, which exists in the element $p = q$, a special treatment is necessary. As is shown in Fig. 3, this area is divided into the following three regions:

- 1) $r_p - \epsilon_0 < \rho < r_p + \epsilon_0$ ($0 < \epsilon < \beta_1, \beta_2$) and $-\gamma < \theta < \gamma$ ($0 < \gamma < 1$), which include the singular point $\rho = r_p$ $\theta = 0$, (double hatched region)
- 2) $r_p - \epsilon_0 < \rho < r_p + \epsilon_0$ but excluding $-\gamma < \theta < \gamma$, (dotted region)
- 3) $r_p - \beta_1 < \rho < r_p - \epsilon_0$ and $r_p + \epsilon_0 < \rho < r_p + \beta_2$, (single hatched region)

Designating the contribution of these three regions of K_1 as J_1 , J_2 and J_3 respectively, eq. 24 gives

$$J_1 = \lim_{\delta \rightarrow 0} \int_{r_p - \epsilon_0}^{r_p + \epsilon_0} \int_{-\gamma}^{\gamma} -\frac{\partial^2}{\partial x^2} \frac{e^{-iq\theta}}{\sqrt{x^2 + r^2 + \rho^2 - 2\rho r \cos \theta}} d\theta d\rho \quad (30)$$

$$J_2 = \lim_{\delta \rightarrow 0} \int_{r_p - \epsilon_0}^{r_p + \epsilon_0} \left[\int_{-\bar{\theta}_b}^{-\gamma} + \int_{+\gamma}^{1/2\bar{\theta}_0} + \sum_{n=1}^N \int_{\bar{\theta}_n - \bar{\theta}_b}^{\bar{\theta}_n + 1/2\bar{\theta}_0} \right] \frac{-\partial^2}{\partial x^2} \frac{e^{-iq\theta}}{\sqrt{X^2 + r^2 + \rho^2 - 2r\rho \cos\theta}} d\theta \quad d\rho \quad (31)$$

$$J_3 = \lim_{X \rightarrow 0} \left[\int_{-r_p - \beta_1}^{r_p - \epsilon_0} + \int_{r_p + \epsilon_0}^{r_p + \beta_2} \right] \sum_{n=1}^N \int_{\bar{\theta}_n - \bar{\theta}_b}^{\bar{\theta}_n + 1/2\bar{\theta}_0} \frac{-\partial^2}{\partial x^2} \frac{e^{-iq\theta}}{\sqrt{X^2 + r^2 + \rho^2 - 2r\rho \cos\theta}} d\theta \quad d\rho \quad (32)$$

The most convenient form for evaluating the total contribution J of these three parts is the limit value expression:

$$J = \lim_{\epsilon_0 \rightarrow 0} (J_1 + J_2 + J_3) \quad (33)$$

As is seen in Appendix D:

$$\lim_{\epsilon_0 \rightarrow 0} J_1 = \lim_{\epsilon_0 \rightarrow 0} \left[-\frac{4}{r_p \epsilon_0} \right] \quad (34)$$

The integrand of J_2 is finite through the whole integration range, and hence

$$\lim_{\epsilon_0 \rightarrow 0} J_2 = 0 \quad (35)$$

In Appendix E, J_3 is given in the following form:

$$\lim_{\epsilon \rightarrow 0} J_3 = \lim_{\epsilon \rightarrow 0} \left[\frac{4}{r_p \epsilon_0} \right] + \frac{2}{(r_p)^2} \left[-\frac{1}{k_1^*} + k_1^* \ln \left(\frac{k_1^*}{4} \right) (B_q - 1/2) \right. \\ \left. + k_1^* \left(A_q - B_q + \frac{1}{4} + \frac{(-1)^{q+1}}{2} \overline{I_q^*} \right) \right] \quad (36)$$

where β_1 and β_2 should be taken to satisfy the relation

$$k_1^* = \frac{\beta_1}{2r_p - \beta_1} = \frac{\beta_2}{2r_p + \beta_2}, \quad (37)$$

where

$$\overline{I_q^*} = \left(- \int_0^{-1/2(\pi - \bar{\theta}_b)} - \int_{-1/2(\pi + \bar{\theta}_o/2)}^{-\pi} + \sum_{n=2}^N \int_{-1/2(\pi + \bar{\theta}_n - \bar{\theta}_b)}^{-1/2(\pi + \bar{\theta}_n + \bar{\theta}_o/2)} \right) \\ \frac{e^{i2q\psi} d\psi}{\sqrt{1 - \sin^2 \psi}}^a$$

A_q , B_q and I_q are given in Appendix D.

An important cancellation occurs between $\lim_{\epsilon \rightarrow 0} J_1$ and the first term of $\lim_{\epsilon \rightarrow 0} J_3$.

K_2 . No singularity is involved in K_2 . Taking the limit value before integration and replacing the summation with integration

$$K_2 = \int_{m=1/2}^{\infty} \int_{\theta=0}^{2\pi} - \left[\frac{\partial^2}{\partial x^2} \frac{e^{-iq\theta}}{\sqrt{X^2 + r^2 + \rho^2 - 2r\rho \cos \theta}} \right] \frac{d\theta}{X = m(1/a) \bar{\theta}_o} dm \\ = - \frac{a}{\bar{\theta}_o} \left[\frac{\partial}{\partial x} \int_{\theta=0}^{2\pi} \frac{e^{-iq\theta}}{\sqrt{X^2 + r^2 + \rho^2 - 2r\rho \cos \theta}} d\theta \right] \Bigg|_{X = \frac{1}{2a} \bar{\theta}_o}^{\infty} \quad (38)$$

Using the Lipschitz integral⁶ and Neumann's addition theorem⁷

$$\begin{aligned}
 G &= \int_0^{2\pi} \frac{e^{-iq\Theta}}{\sqrt{X^2+r^2+\rho^2-2r\rho\cos\Theta}} d\Theta \\
 &= \int_{\Theta=0}^{2\pi} e^{-iq\Theta} \int_{k=0}^{\infty} e^{-|X|k} \sum_{m=0}^{\infty} \epsilon_m J_m(kr) J_m(k\rho) \cos m\Theta dk d\Theta,
 \end{aligned} \tag{39}$$

where

$$\epsilon_m = \begin{cases} 1 & \text{for } m = 0 \\ 2 & \text{for } m \neq 0 \end{cases}$$

Further,

$$\begin{aligned}
 G &= 2\pi \int_{k=0}^{\infty} J_q(kr) J_q(k\rho) e^{-|X|k} dk \\
 &= \frac{2}{\sqrt{r\rho}} Q_{q-1/2}(Z) \quad (\text{ref. 8})
 \end{aligned}$$

where

$$Z = \frac{r^2 + \rho^2 + X^2}{2r\rho} \tag{41}$$

The function $Q_{q-1/2}$ is a spherical function. Numerical tables of $Q_{q-1/2}$ necessary for the following treatment are given in ref. 9.

$$\begin{aligned}
 \frac{\partial}{\partial x} G &= \frac{2}{\sqrt{r\rho}} \frac{\partial}{\partial Z} Q_{q-1/2}(Z) \frac{\partial Z}{\partial x} \\
 &= \frac{2x}{(\sqrt{r\rho})^3} \frac{q-1/2}{Z^2-1} \left[Z Q_{q-1/2}(Z) - Q_{q-3/2}(Z) \right]
 \end{aligned} \tag{42}$$

The behavior of $Q_{n-1/2}$ for large Z is

$$Q_{n-1/2} = 1/2 \sum_{s=0}^{\infty} \frac{\Gamma^2(n+s+1/2)}{s! (n+s)!} \left(\frac{Z}{Z+1}\right)^{n+s+1/2} \quad (43)$$

Hence in the present problem with $q \geq 0$,

$$\left[\frac{\partial}{\partial x} G \right]_{x=\infty} = 0 \quad (44)$$

Thus, finally

$$K_2 = \frac{1}{(\sqrt{r\rho})^3} \frac{q-1/2}{Z_o^{2-1}} \left[Z_o Q_{q-1/2}(Z_o) - Q_{q-3/2}(Z_o) \right]$$

$$\text{where } Z_o = \frac{r^2 + \rho^2 + \left(\frac{1}{2a} \bar{\theta}_o\right)^2}{2r\rho} \quad (45)$$

NUMERICAL RESULTS AND DISCUSSION

Calculations have been performed to assess the theoretical approach evolved here and to determine the three-dimensional effects in the stationary and nonstationary flow cases as well as the effects of such important parameters as blade-area ratio and pitch angle. The calculations have been restricted to a four-blade propeller with sector type blade form and blade-area ratios $A_B = 0.22, 0.44$ and 0.66 and to a constant amplitude gust velocity from root to tip expressed by $W = W_0 e^{-iq\phi}$.

The results are exhibited in Figs. 4, 5 and 6 and summarized in Table I for frequencies $q = 0$ to 4 and for representative values of inverse pitch angle, a , which bracket the range of pitch-diameter ratio of practical interest; i.e., $a = 2\pi$, $P/D = 1/2$ and $a = \pi$, $P/D = 1$. In the same figures the results of calculations for Weissinger's two-dimensional model by a stripwise method are presented for comparison.

As a measure of the three-dimensional effect, $R_{3/2}$ is introduced to indicate the ratio of the three-dimensional results for total lift to the corresponding two-dimensional value:

$$R_{3/2} = \frac{\text{load by three-dimensional calculation}}{\text{load by stripwise two-dimensional approach}}$$

Since the three-dimensional and two-dimensional results are obtained through the same Weissinger approximation, $R_{3/2}$ can be said to be a well-defined measure of the three-dimensional effect.

It is seen from Figs. 4, 5 and 6 that the ratio $R_{3/2}$ decreases for decreasing order of harmonic q . This indicates that the over-all correction for three-dimensional

effects is much more pronounced in the stationary case than in unsteady flow, a fact which can be explained at least qualitatively, in the following manner. The propeller, as any other lifting surface of finite aspect ratio, is accompanied by two free vortex systems. As a result of the spanwise gradient of the circulation, a free vortex system is developed along the helicoidal surface. On the other hand, the timewise change of circulation leads to a radial free vortex system. The first system is characteristic only of three-dimensional flow conditions whereas the second is present as well in the two-dimensional model and to the same extent. In the marine propeller case due to high load and rather low pitch, the effect of the first vortex system is heavily accumulated in stationary flow conditions, thus there is a large discrepancy between two and three-dimensional results. In nonstationary flow conditions the helical free vortex changes sign q times per pitch and hence the accumulated effect is mitigated considerably. The higher the frequency the smaller the effect of the helical free vortices, therefore the closer the three-dimensional results to the corresponding two-dimensional case.

The results also indicate that for higher blade-area ratio, i.e., for wider blade where the interaction between blades becomes greater, the three-dimensional effect is more pronounced. In fact, Fig. 7 shows that for larger blade-area ratio, coincidence of the results by both approaches, three-dimensional and two-dimensional, will be delayed to higher reduced frequencies. As the area ratio decreases, coincidence will occur at lower reduced frequencies; in other words, three-dimensional effects become less important. The effect of inverse pitch angle, α , is not as important (in the range $\pi \leq \alpha \leq 2\pi$) as is the blade-area ratio. However, it can be said that the smaller α the closer the three-dimensional load to the two-dimensional value.

For an airscrew propeller with small blade-area ratio (small solidity) and high pitch angle (small α) the three-dimensional effects should be less important than for the marine propeller with larger area ratio and smaller pitch angle. This conclusion is borne out also by the comparison on the same figures of the phase angles between downwash velocity and loading obtained by both approaches. It is seen that as the order of harmonics increases, the three-dimensional value for the phase angle tends towards the corresponding value for the two-dimensional case. For smaller blade-area ratio, the deviation is minimized at lower reduced frequencies.

On the basis of the present investigation revision can now be made of the method used in ref. 3 to obtain vibratory thrust and torque and the large discrepancy shown there between theoretical and experimental results can be explained. The method of ref. 3 was based on the work of Ritger and Breslin² who used two-dimensional unsteady airfoil theory in a stripwise fashion in conjunction with Burrill's semi-empirical correction factors.¹¹ Burrill's corrections, which include among others those for three-dimensional effects, are determined for stationary flow (steady-state) only. Use of these corrections in refs. 2 and 3 for both steady and unsteady flow is now proved invalid. The fact that the calculated load amplitude in unsteady flow was found to be 1/3 of the experimental value can now be explained by the results of the present theory which show that the correction factor for three-dimensional effects is quite different for stationary ($q = 0$) and nonstationary cases. From the figures and Table I, it is seen that

$$\frac{R_{3/2} \text{ for } q = 0}{R_{3/2} \text{ for } q = 4} \sim \frac{1}{3}$$

which indicates that the values of the unsteady loads obtained by the method of ref. 3 were overcorrected. If the

right correction factor were used in the unsteady two-dimensional approach the theoretical result would have been closer to experiment.

CONCLUSIONS

The unsteady lifting surface integral equation is derived for the marine propeller case and its solution obtained by using the Weissinger approximation. The kernel function is expressed in closed form after some mathematical simplification. The applicability of the Weissinger method for the nonstationary flow case is studied and the results indicate the validity of the method up to reduced frequency 1.3 which corresponds to the blade frequency of a four-bladed propeller of area ratio about 0.4 and of a three-bladed propeller of area ratio of 0.6.

The numerical examples restricted to a four-blade propeller with sector type of blade form of area ratio 0.22, 0.44 and 0.66 and to a constant amplitude gust show that the difference between the three-dimensional approach and the two-dimensional stripwise approach diminishes as the order of harmonic increases, as the area ratio of the blade decreases and with increasing pitch-diameter ratio.

ACKNOWLEDGMENTS

The authors wish to express their indebtedness to Dr. J. Breslin for his valuable discussions and suggestions during the development of the present work, and to Miss W. R. Jacobs and Mr. K. Eng for their assistance in calculations and preparation of this report.

REFERENCES

1. Sears, W. R.: "Some Aspects of Nonstationary Airfoil Theory and its Practical Application," Jour. Aer. Sci. Vol. 8, No. 3, 1941, p. 104f.
2. Ritger, P. D. and Breslin, J. P.: "A Theory of the Quasi-Steady and Unsteady Thrust and Torque of a Propeller in a Ship Wake," DL Report 686, 1958.
3. Tsakonas, S. and Jacobs, W.R.: "Theoretical Calculations of Vibratory Thrust and Torque and Comparisons with Experimental Measurements," DL LR-827, 1961.
4. Sparenberg, J. A.: "Application of Lifting Surface Theory to Ship Screws," Koninkel. Nederl. Academie van Wetenschappen - Amsterdam, Proceed. Series B, 62, No. 5, 1959, p. 286f.
5. Hanaoka, T.: "Introduction to the Nonuniform Hydrodynamics Concerning a Screw Propeller," Jour. Zosenkyokai, Japan, No. 109, p. 1f and "On the Integral Equation Concerning an Oscillating Screw Propeller by Lifting Line Theory," Ibid No. 110, p. 185f.
6. Watson, G. N.: "Theory of Bessel Functions," Cambridge at the University Press, 1952, p. 384.
7. Watson, G. N.: "Theory of Bessel Functions," Cambridge Univ. Press, 1952, p. 358.
8. Watson, G. N.: "Theory of Bessel Functions," Cambridge Univ. Press, 1952, p. 389.
9. Sluyter, M. M.: "A Computational Program and Extended Tabulation of Legendre Functions of Second Kind and Half-order," Therm Advanced Research, TAR-TR 601, August 1960.
10. Watkins, Charles: Unpublished letter
11. Burrill, L. C.: "Calculation of Marine Propeller Performance Characteristics," North-East Coast Inst. of Eng. and Shipbuilders, March 1944, p. 264.

TABLE I
SUMMARY OF RESULTS FOR $R_{3/2}$ AND CORRESPONDING PHASE
ANGLES, FOR FOUR-BLADE PROPELLERS OF DIFFERENT
BLADE-AREA RATIO AND INVERSE PITCH ANGLES

A) Values of $R_{3/2}$											
$A_B = 0.22$						$A_B = 0.44$					
q	k	a=2 π	a=3 $\pi/2$	a= π	k	a=2 π	a=3 $\pi/2$	a= π	k	a=2 π	a=3 $\pi/2$
0	0	.258	.284	.314	0	.145	.162	.182	0	.102	.115
1	.173	.336	.373	.410	.346	.243	.270	.300	.518	.199	.222
2	.346	.414	.450	.489	.691	.338	.371	.407	1.036	.293	.323
3	.518	.468	.504	.539	1.036	.412	.447	.480	1.554	.380	.412
4	.691	.534	.570	.603	1.382	.496	.532	.564	2.073	.479	.513
B) Phase Angle Difference at 0.7 Radius											
1	.173	14.1°	13.8°	13.5°	.346	16.9°	16.6°	16.5°	.518	16.1°	16.1°
2	.346	13.6°	13.2°	12.8°	.691	12.6°	12.3°	12.1°	1.036	8.2°	8.1°
3	.518	10.8°	10.3°	9.8°	1.036	6.6°	6.3°	6.1°	1.554	2.9°	2.9°
4	.691	7.7°	7.2°	6.7°	1.382	1.9°	1.8°	1.6°	2.073	-0.2°	-0.3°
											16.0°
											8.0°
											2.8°
											-0.3°

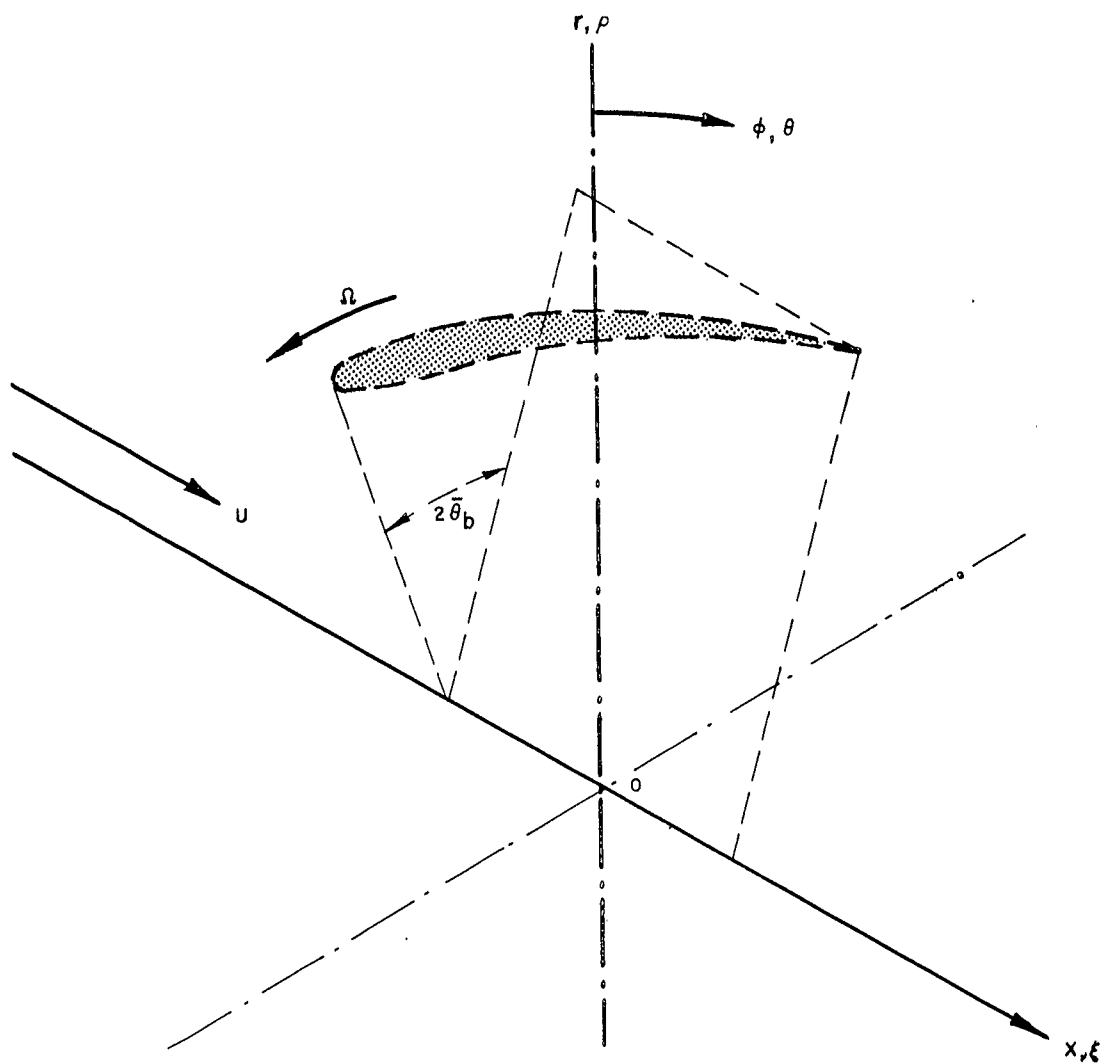


FIGURE 1. COORDINATE SYSTEM AND NOTATIONS

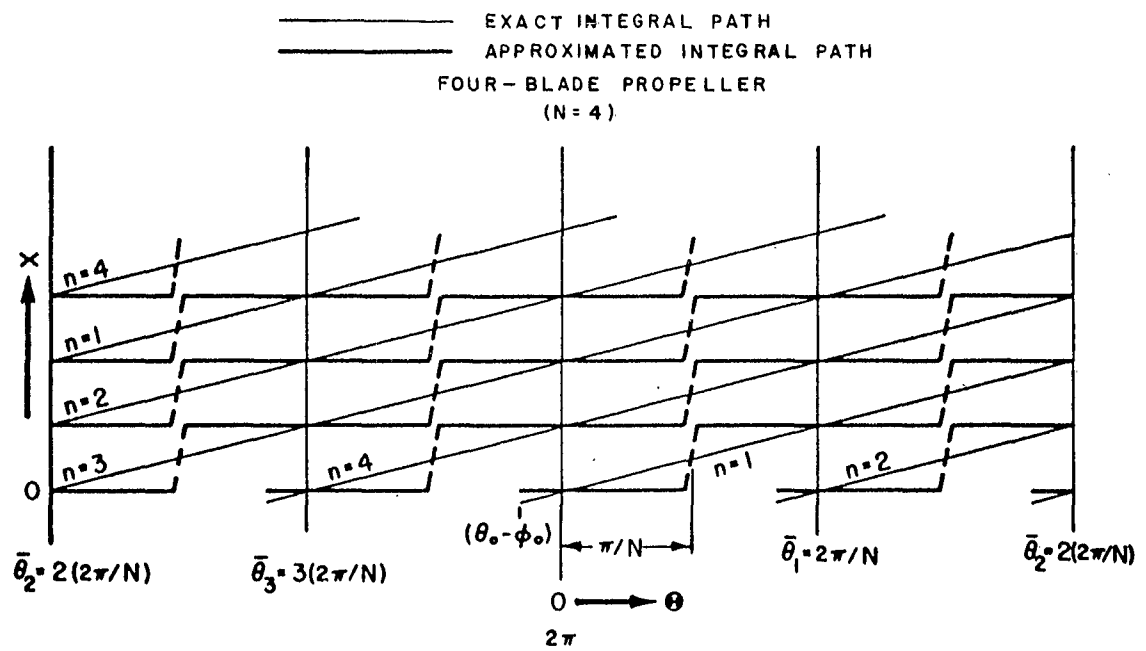


FIGURE 2. APPROXIMATION OF INTEGRAL PATH

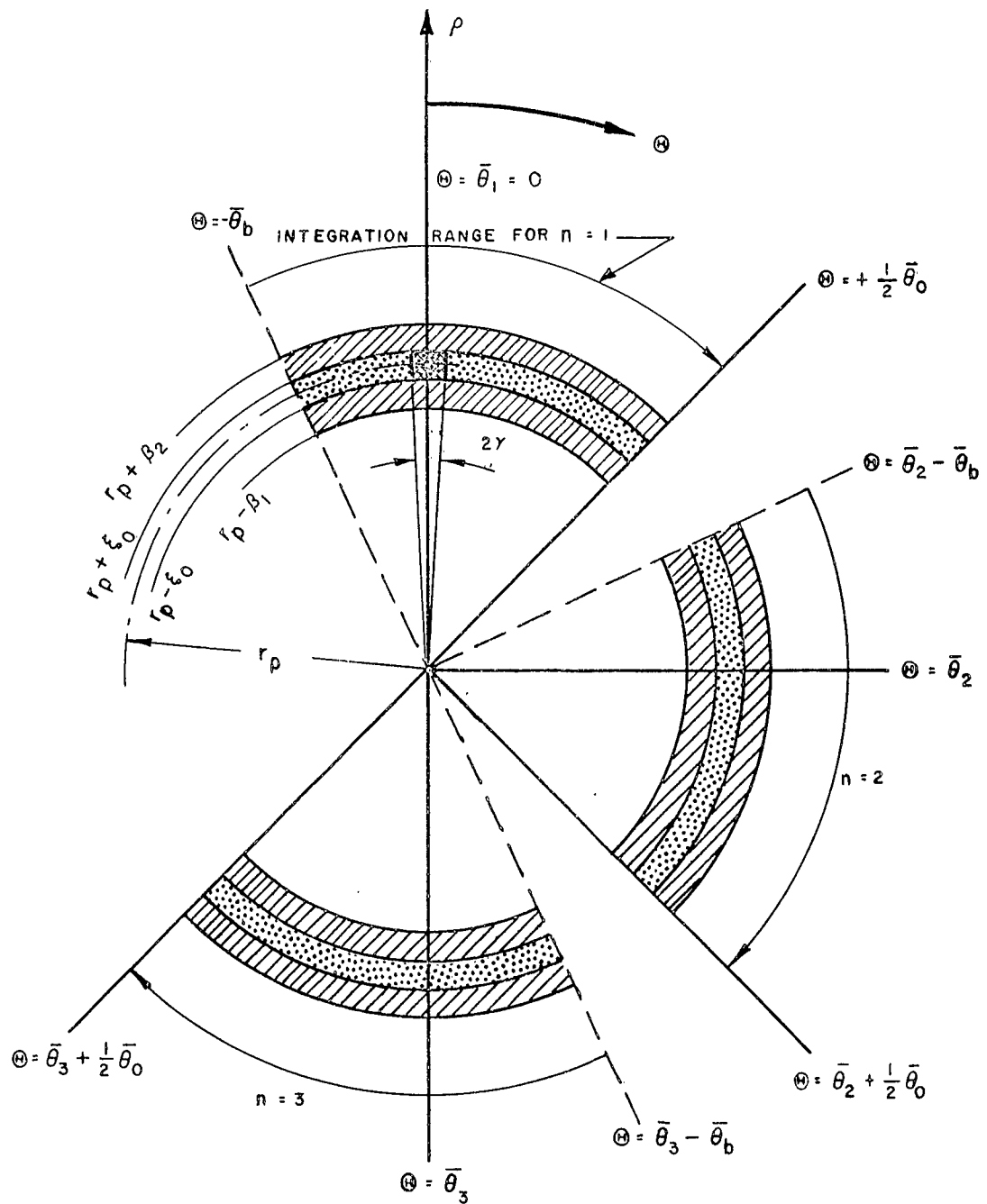


FIGURE 3. DOMAINS OF INTEGRATION

4-BLADE PROPELLER WITH SECTOR FORM BLADES

PROJECTED AREA RATIO = 0.44

HUB RADIUS/PROPELLER RADIUS = 0.3

GUST: $w = w_0 e^{-iq\phi}$

w_0 = CONSTANT

ϕ = ANGULAR COORDINATE FIXED IN BLADE

q = ORDER OF HARMONIC

LOAD: $|L|e^{i\beta} = (L_0/w_0)(1/4\pi\mu\alpha U_0^2)$

r_0 = PROPELLER RADIUS

μ = FLUID DENSITY

U = FREE-STREAM VELOCITY

α = INVERSE PITCH ANGLE

β_2, β_3 = PHASE ANGLE IN TWO AND THREE

DIMENSIONAL CASES

$R_3 = \frac{\text{LOAD BY 3-DIM. CALCULATION}}{\text{LOAD BY 2-DIM. STRIPWISE METHOD}}$

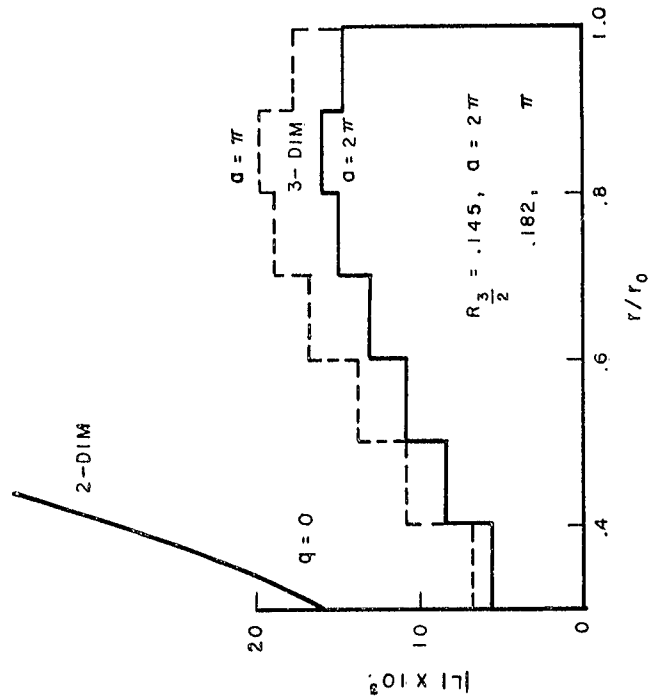
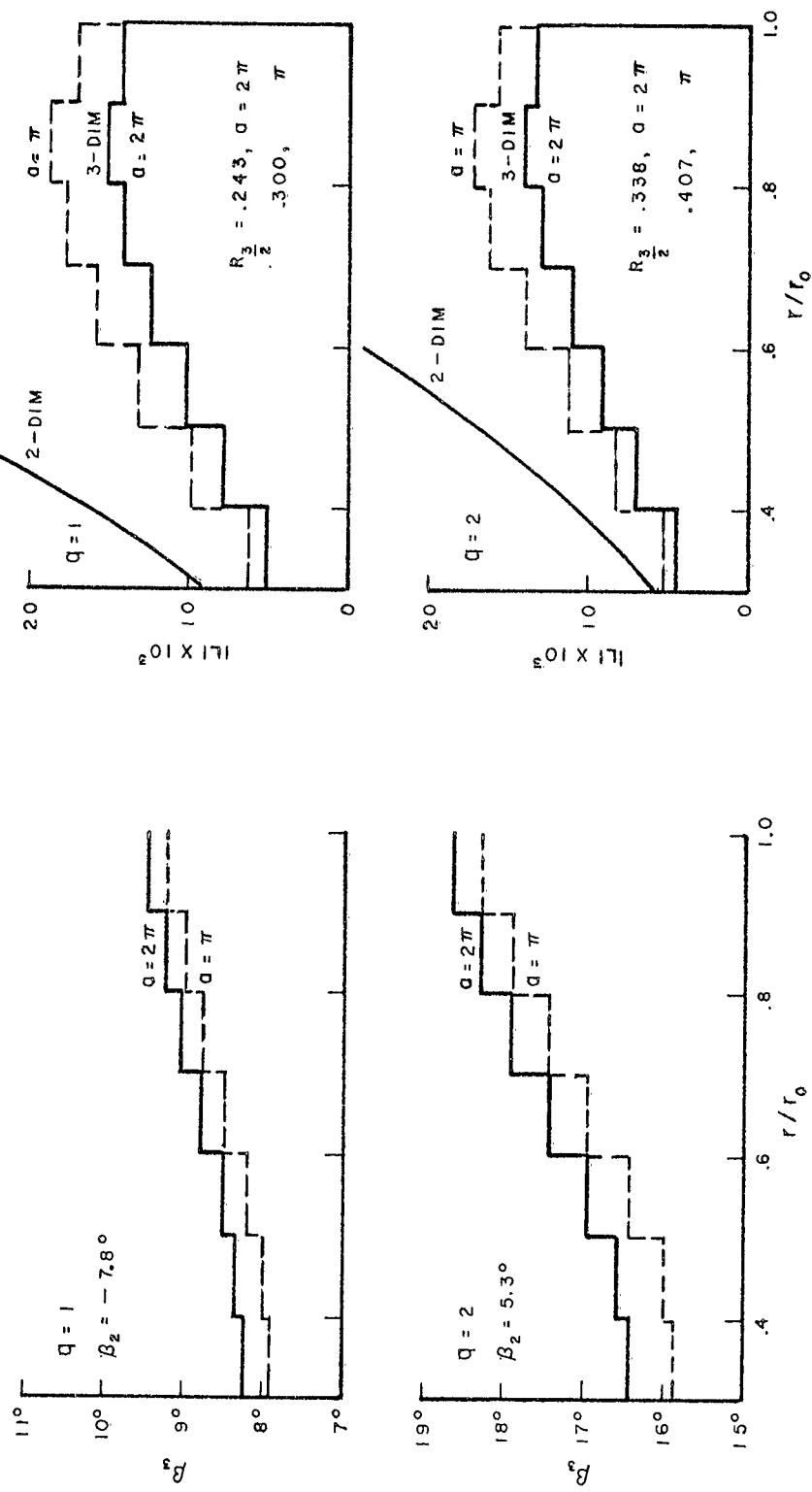
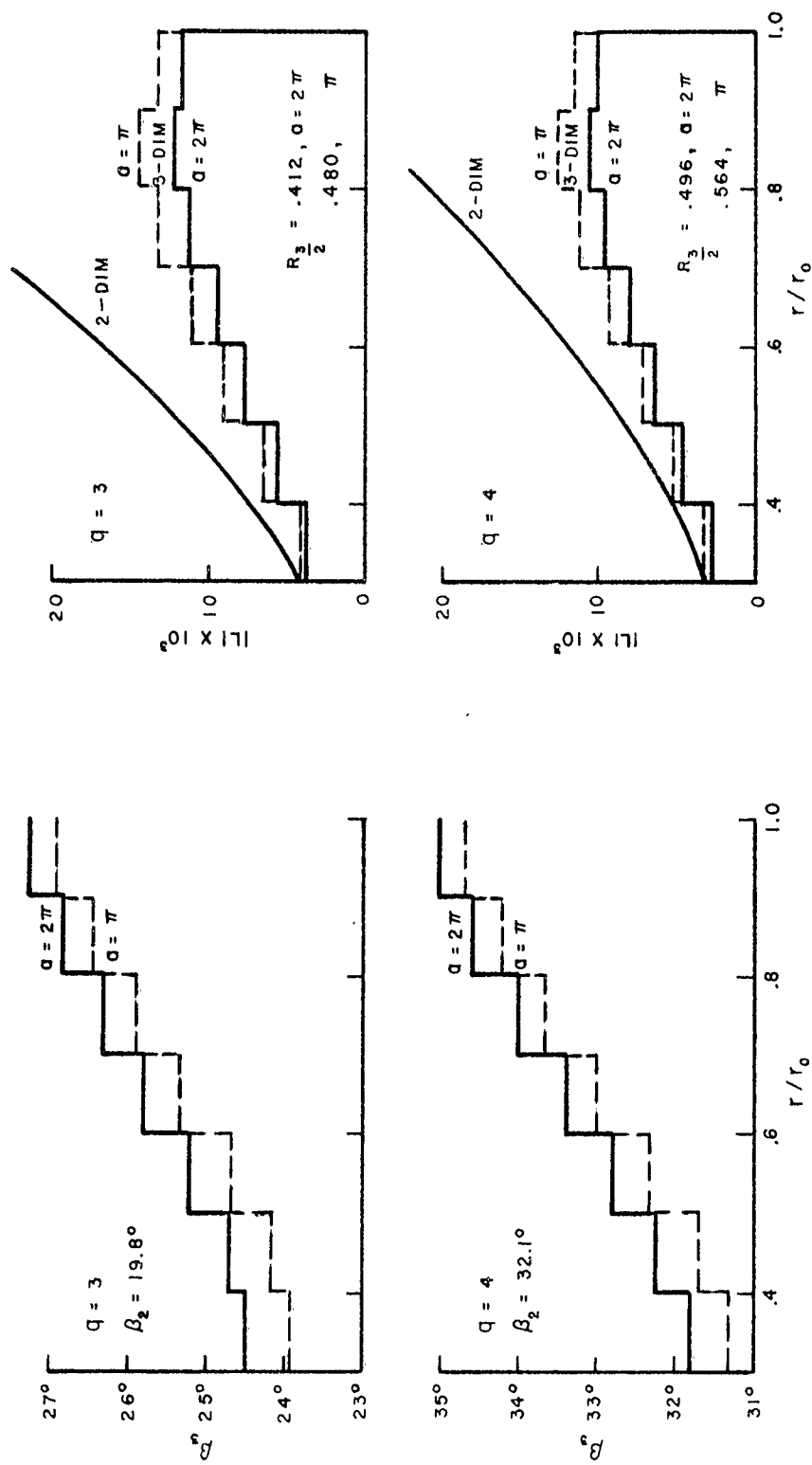


FIGURE 4a. SPANWISE LOAD AND PHASE ANGLE DISTRIBUTIONS FOR TWO-DIMENSIONAL AND THREE-DIMENSIONAL WEISSINGER MODELS



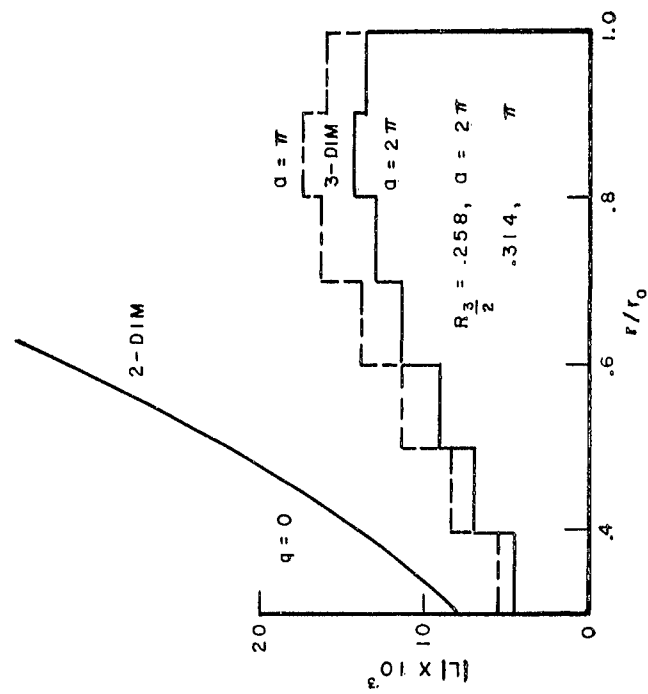
R-940

FIGURE 4b. SPANWISE LOAD AND PHASE ANGLE DISTRIBUTIONS FOR TWO-DIMENSIONAL AND THREE-DIMENSIONAL WEISSINGER MODELS



R-940

FIGURE 4c. SPANWISE LOAD AND PHASE ANGLE DISTRIBUTIONS FOR TWO-DIMENSIONAL AND THREE-DIMENSIONAL WEISINGER MODELS



4-BLADE PROPELLER WITH SECTOR FORM BLADES

PROJECTED AREA RATIO = 0.22

SEE FIGURE 4a FOR LEGEND

FIGURE 5a. SPANWISE LOAD AND PHASE ANGLE DISTRIBUTIONS FOR TWO-DIMENSIONAL AND THREE-DIMENSIONAL WEISSINGER MODELS

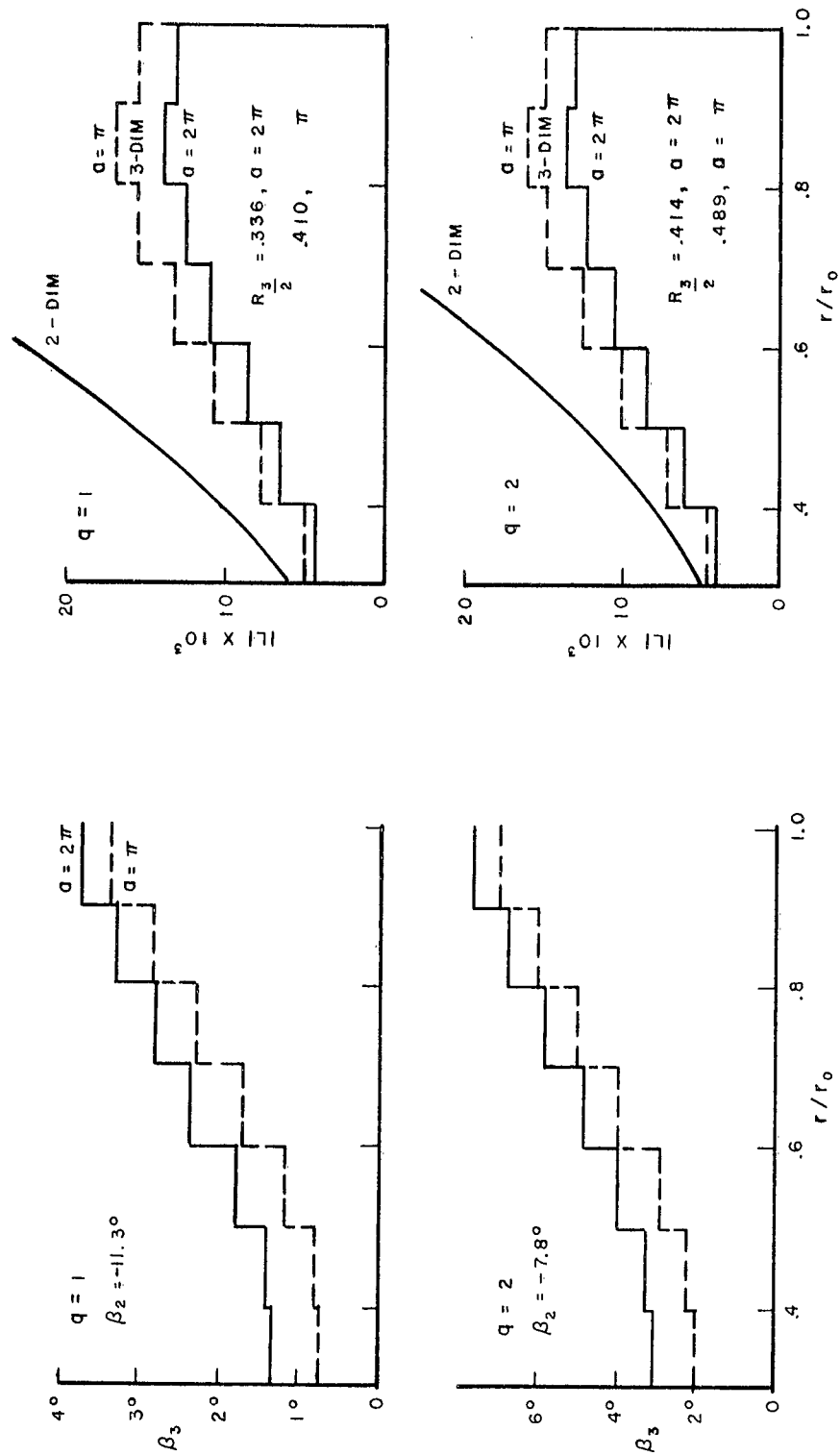


FIGURE 5b. SPANWISE LOAD AND PHASE ANGLE DISTRIBUTIONS FOR TWO-DIMENSIONAL AND THREE-DIMENSIONAL WEISSINGER MODELS

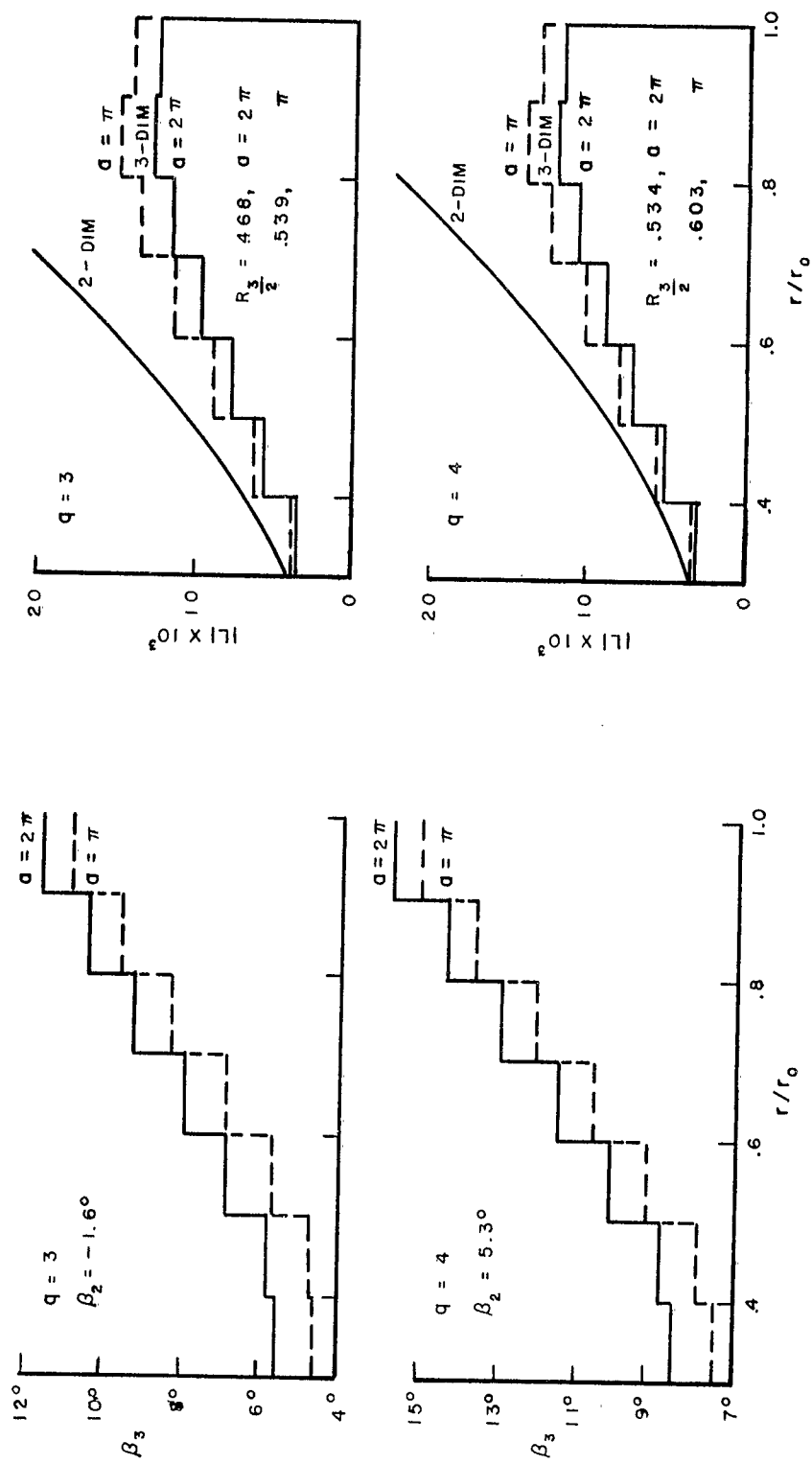
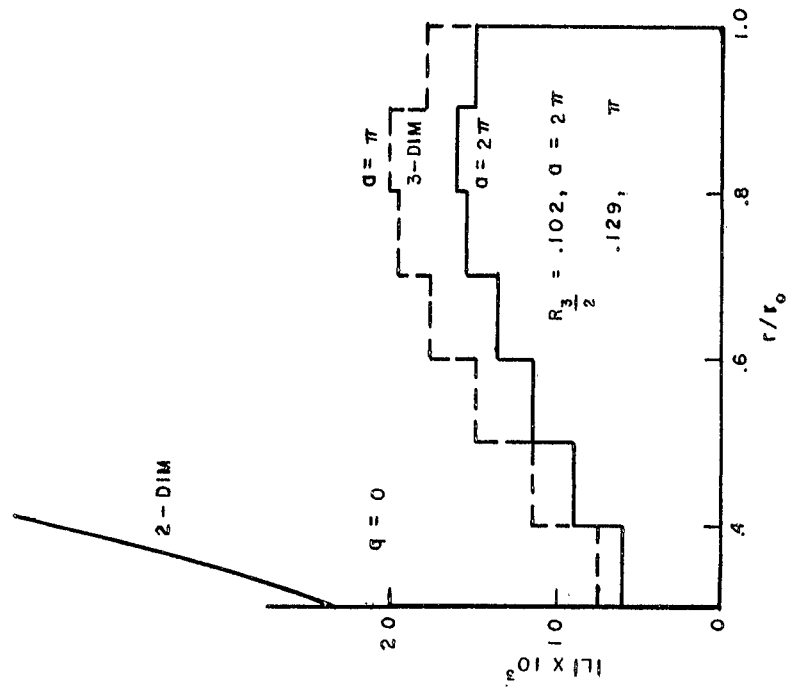


FIGURE 5c. SPANWISE LOAD AND PHASE ANGLE DISTRIBUTIONS FOR TWO-DIMENSIONAL AND THREE-DIMENSIONAL WEISSINGER MODELS



4-BLADE PROPELLER WITH SECTOR FORM BLADES

PROJECTED AREA RATIO = 0.66

SEE FIGURE 4a FOR LEGEND

FIGURE 6a. SPANWISE LOAD AND PHASE ANGLE DISTRIBUTIONS FOR TWO-DIMENSIONAL AND THREE-DIMENSIONAL WEISSINGER MODELS

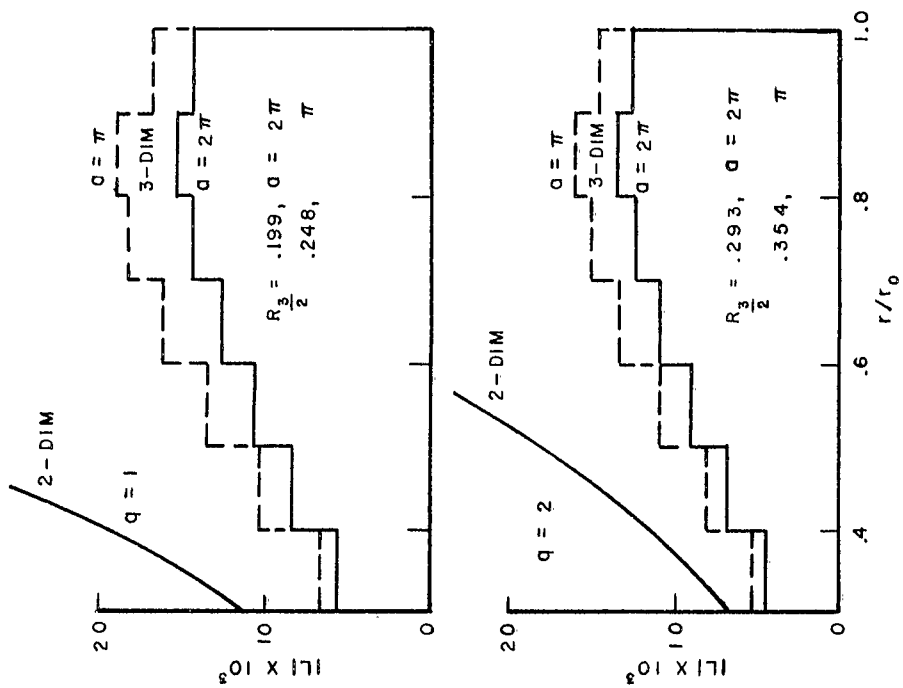
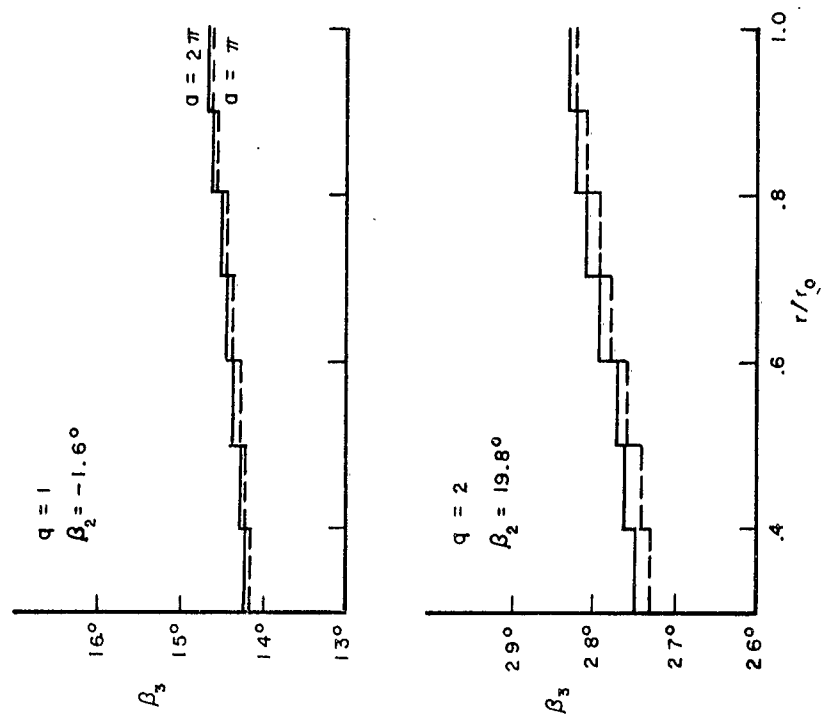


FIGURE 6b. SPANWISE LOAD AND PHASE ANGLE DISTRIBUTIONS FOR TWO-DIMENSIONAL AND THREE-DIMENSIONAL WEISSINGER MODELS

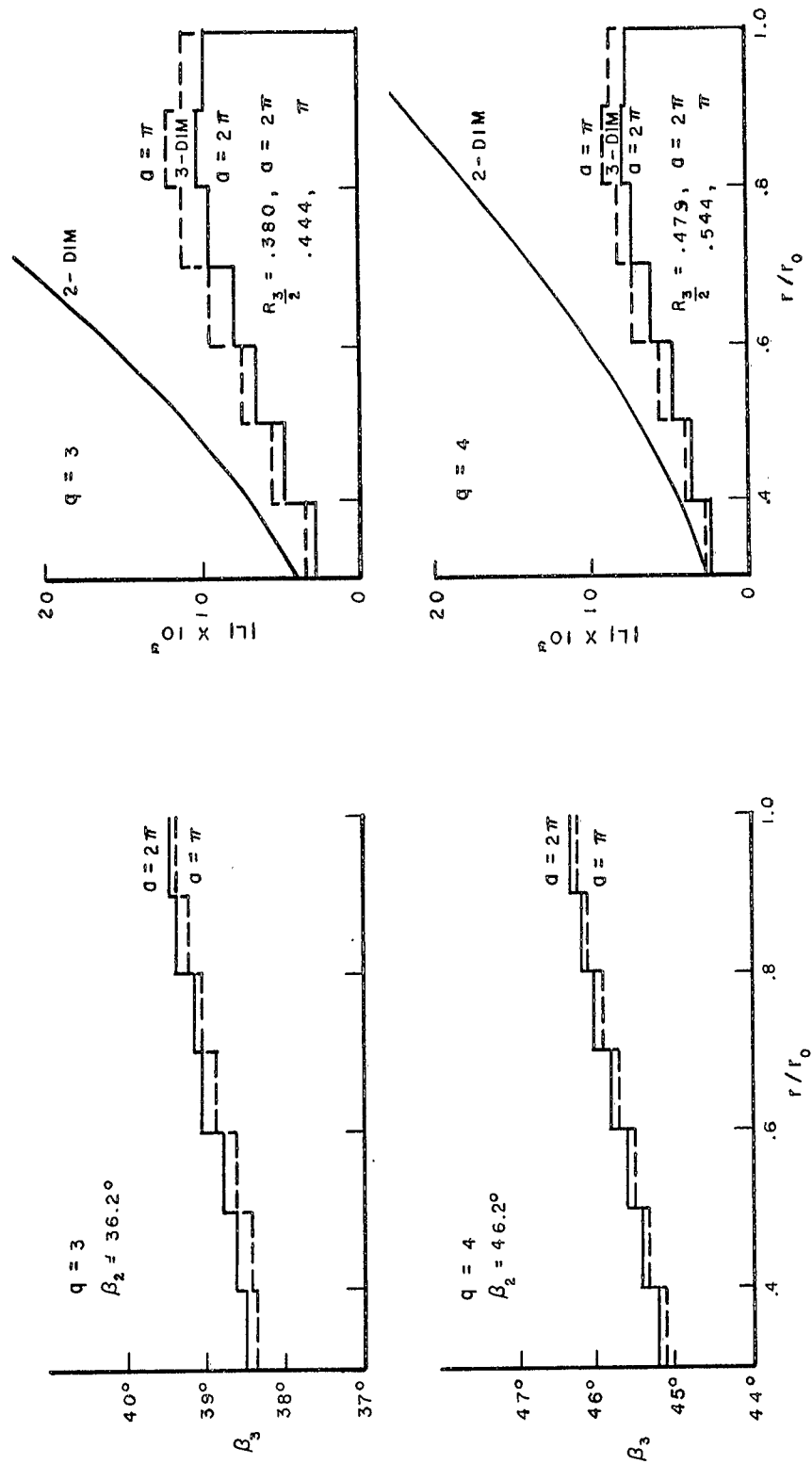


FIGURE 6c. SPANWISE LOAD AND PHASE ANGLE DISTRIBUTIONS FOR TWO-DIMENSIONAL AND THREE-DIMENSIONAL WEISSINGER MODELS

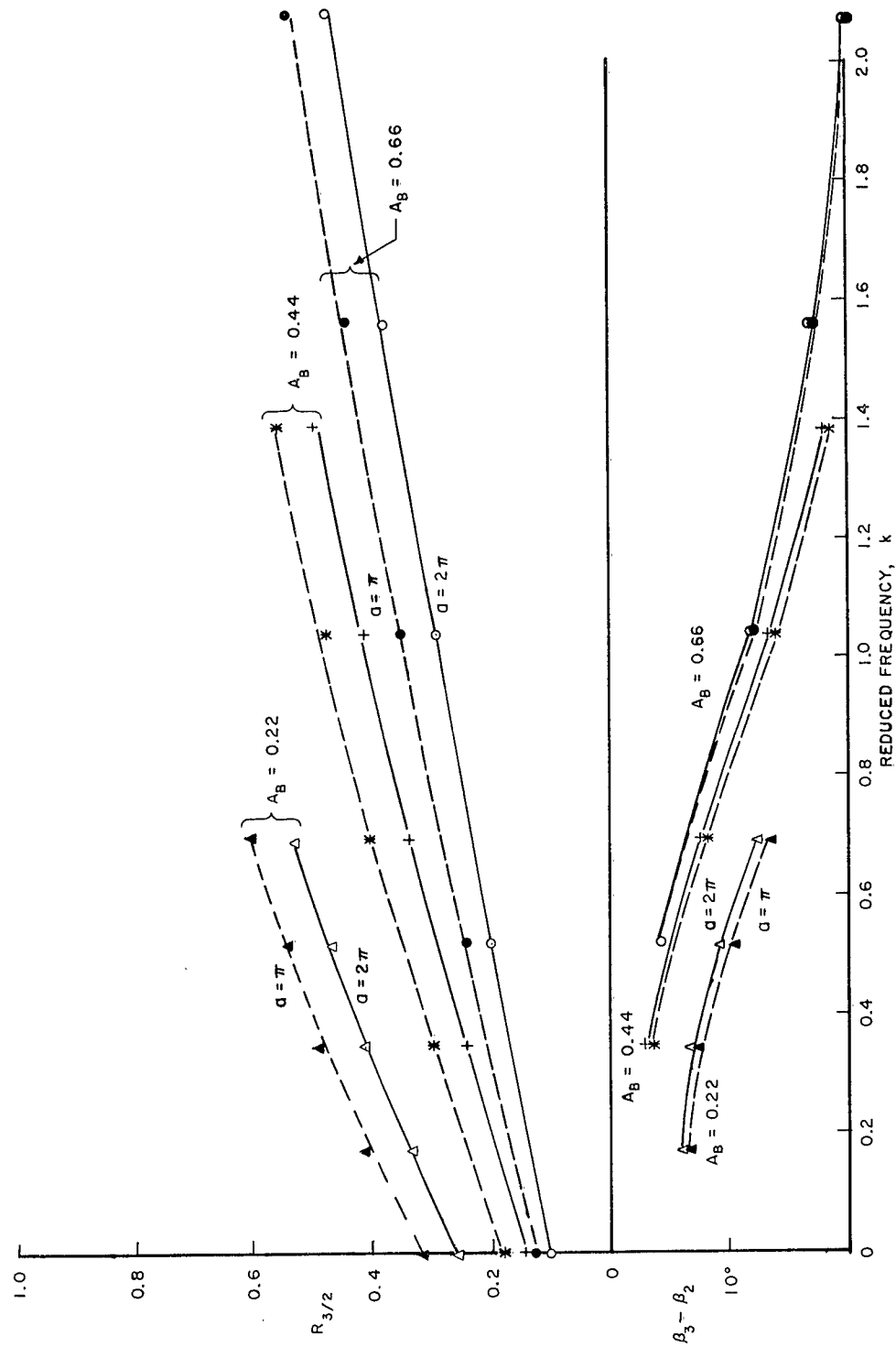


FIGURE 7. THREE-DIMENSIONAL CORRECTION FACTOR $R_{3/2}$ AND PHASE-ANGLE DIFFERENCE BETWEEN THREE AND TWO-DIMENSIONAL ANALOGS AT 0.7 RADIUS VERSUS REDUCED FREQUENCY AT VARIOUS BLADE AREA RATIOS FOR $\alpha = \pi$ AND 2π

APPENDIX A.
APPLICABILITY OF THE WEISSINGER METHOD
TO THE NONSTATIONARY PROBLEM

In order to clarify the applicability of the Weissinger method to nonstationary problems, Sears' sinusoidal gust problem is treated by this method in this section.

Consider the system shown in Fig. A-1. The induced velocity due to a pulsating dipole located at (x', y', z') is obtained in the way described in "Formulation of Problem," (eqs. 1 to 8).

$$W(x, y, z, t) = \frac{e^{i\omega t}}{4\pi\mu U} \frac{\partial}{\partial z} \frac{\partial}{\partial z'} \int_{-\infty}^{x-x'} e^{i\frac{\omega}{U}(\tau-x+x')} \cdot \frac{1}{\sqrt{\tau^2 + (y-y')^2 + (z-z')^2}} d\tau \quad (A-1)$$

It must be noted here that the dipole axis is taken in the negative z' -direction so that the positive direction of the lift will coincide with positive z' . If the dipoles are distributed uniformly from $y' = -\infty$ to $y' = +\infty$ on the $1/4$ -chord line, the induced velocity upon the $3/4$ -chord line is

$$W(t) = \lim_{Z \rightarrow 0} \frac{L_0 e^{i\omega t}}{4\pi\mu U} \int_{Y=-\infty}^{+\infty} \frac{-\partial^2}{\partial Z^2} \int_{\tau=-\infty}^{+1} e^{ik(\tau-1)} \frac{1}{\sqrt{\tau^2 + Y^2 + Z^2}} d\tau dY \quad (A-2)$$

where L_0 is the lift per span and $k = \frac{\omega}{U}$ is the reduced frequency. The integral part of eq. A-2 is written as

$$\begin{aligned} G &= \lim_{Z \rightarrow 0} \int_{Y=-\infty}^{+\infty} \frac{-\partial^2}{\partial Z^2} \int_{\tau=-\infty}^{+1} e^{ik\tau} \frac{1}{\sqrt{\tau^2 + Y^2 + Z^2}} d\tau dY \\ &= \lim_{Z \rightarrow 0} \frac{\partial}{\partial Z} \int_{\tau=-\infty}^1 e^{ik\tau} \frac{2Z}{\tau^2 + Z^2} d\tau \end{aligned} \quad (A-3)$$

G is divided into three parts:

$$G = 2(G_1 + G_2 + G_3)$$

$$G_1 = \lim_{Z \rightarrow 0} \frac{\partial}{\partial Z} \int_{-\infty}^{-\epsilon} e^{ik\tau} \frac{Z}{\tau^2 + Z^2} d\tau$$

$$G_2 = \lim_{Z \rightarrow 0} \frac{\partial}{\partial Z} \int_{-\epsilon}^{+\epsilon} e^{ik\tau} \frac{Z}{\tau^2 + Z^2} d\tau$$

$$G_3 = \lim_{Z \rightarrow 0} \frac{\partial}{\partial Z} \int_{+\epsilon}^{+1} e^{ik\tau} \frac{Z}{\tau^2 + Z^2} d\tau \quad (A-4)$$

where it is assumed that $|\epsilon| \ll 1$.

Since the integration range of G_1 includes no singularity, $\left(\lim_{Z \rightarrow 0} \frac{\partial}{\partial Z}\right)$ can be taken before integration, and G_1 is obtained in the following form:

$$\begin{aligned} G_1 &= \int_{-\infty}^{-\epsilon} e^{ik\tau} \frac{1}{\tau^2} d\tau \\ &= \frac{1}{\epsilon} \cos k\epsilon - k\frac{\pi}{2} + k\text{Si}(k\epsilon) - i\frac{1}{\epsilon} \sin(k\epsilon) + ik\text{Ci}(k\epsilon) \quad (A-5) \end{aligned}$$

where Ci and Si are the cosine and sine integrals which are given by

$$\text{Ci}(x) = - \int_x^{\infty} \frac{\cos t}{t} dt$$

$$\text{and } \text{Si}(x) = \int_0^x \frac{\sin t}{t} dt, \text{ respectively.}$$

In a similar way,

$$G_3 = \int_{\epsilon}^1 \frac{e^{ik\tau}}{\tau^2} d\tau$$

$$= -\cos k + \frac{1}{\epsilon} \cos k\epsilon - k\text{Si}(k) + k\text{Si}(k\epsilon)$$

$$- i \sin k + i \frac{1}{\epsilon} \sin k\epsilon - ik\text{Ci}(k\epsilon) + ik\text{Ci}(k). \quad (\text{A-6})$$

In the integral region of G_2 , there is a singular point. Therefore the limit $Z \rightarrow 0$ must be taken last. The exponential is, in series form,

$$e^{ik\tau} = 1 + ik\tau - \frac{1}{2}(k\tau)^2 \dots \quad (\text{A-7})$$

The contribution of the first term of G_2 is

$$\begin{aligned} G_{21} &= \lim_{Z \rightarrow 0} \frac{\partial}{\partial Z} \int_{-\epsilon}^{+\epsilon} \frac{Z}{\tau^2 + Z^2} d\tau \\ &= -2 \frac{1}{\epsilon} \end{aligned} \quad (\text{A-8})$$

That of the second term (and, in general, the terms of odd powers of τ) is zero; that is,

$$G_{22} = \lim_{Z \rightarrow 0} \frac{\partial}{\partial Z} \int_{-\epsilon}^{+\epsilon} ik\tau \frac{Z}{\tau^2 + Z^2} d\tau = 0 \quad (\text{A-9})$$

The contribution of the third term is

$$\begin{aligned} G_{23} &= \lim_{Z \rightarrow 0} \frac{\partial}{\partial Z} \int_{-\epsilon}^{+\epsilon} -\frac{1}{2}(k\tau)^2 \frac{Z}{\tau^2 + Z^2} d\tau \\ &= -k^2\epsilon \end{aligned} \quad (\text{A-10})$$

Summing up these results and taking the limit as $\epsilon \rightarrow 0$ leads to

$$\begin{aligned} G &= \lim_{\epsilon \rightarrow 0} 2 (G_1 + G_2 + G_3) \\ &= 2 [-e^{ik} + ik(\text{Ci}(k) + i\text{Si}(k) + i \frac{\pi}{2})] \end{aligned} \quad (\text{A-11})$$

which upon substitution into eq. A-2 leads to:

$$W(t) = e^{i\omega t} \frac{-L_o}{2\pi\mu U} [1 - ike^{-ik} (Ci(k) + iSi(k) + i \frac{\pi}{2})] \quad (A-12)$$

If the upwash velocity at 3/4-chord point $V_{3/4}e^{i\omega t}$ is given, the complex amplitude of the lift L_o is obtained by the following equation:

$$V_{3/4} = \frac{L_o}{2\pi\mu U} [1 - ike^{-ik} (Ci(k) + iSi(k) + i \frac{\pi}{2})] \quad (A-13)$$

The upwash velocity distribution is given as $V(x)e^{i\omega t}$ where $V(x)$ may be expanded in Birnbaum's form

$$V(x) = v_o - \sum_{n=1}^{\infty} v_n \cos n\alpha \quad (A-14)$$

and $V_{3/4}$ is obtained by setting $x = 1/2$.

However, when the series $V(x)$ is composed of more than two terms, the straightforward application $V_{3/4} = V(1/2)$ leads to very poor results for the Weissinger method. This difficulty can be overcome by an averaging process: $V_{3/4}$ is taken as

$$V_{3/4} = \frac{1}{\pi} \int_0^{\pi} V(x) (1 - \cos \alpha) d\alpha \quad (A-15)$$

where $x = -\cos \alpha$ and the integral operator $\frac{1}{\pi} \int_0^{\pi} (1 - \cos \alpha) d\alpha$ is nothing but Glauert's lift operator.

If eq. A-15 is used in the stationary state case, the Weissinger approximation gives exactly the same results as thin airfoil theory. On expanding $V(x)$ in Birnbaum's form and applying the Glauert integral operator, it is easily found that the result obtained is the velocity at 3/4-chord point due to the first and the second term components of the

upwash velocity $V(x)$ in the Birnbaum form.

It must be noted once more that the application of the operator gives exact results only in the stationary case. However, in the following, the application of this operator to nonstationary problems is tried..

In Sears' sinusoidal gust problem, the upwash velocity $V(x, t)$ is given in the form of

$$V(x, t) = V_o e^{i\omega(t - \frac{x}{U})} \quad (A-16)$$

and with $x = - \cos \alpha$

$$V(x, t) = V_o e^{i\omega t} e^{ik \cos \alpha} \quad (A-17)$$

where $k = \frac{\omega}{U}$ is reduced frequency. If the integral operator is applied

$$\begin{aligned} V_{3/4} &= V_o \frac{1}{\pi} \int_0^\pi (1 - \cos \alpha) e^{ik \cos \alpha} d\alpha \\ &= V_o \frac{1}{\pi} \int_0^\pi (1 - \cos \alpha) (J_0(k) + 2 \sum_{n=1}^{\infty} i^n J_n(k) \cos n\alpha) d\alpha \\ &= V_o [J_0(k) - iJ_1(k)] \end{aligned} \quad (A-18)$$

On substituting in eq. A-13:

$$V_o [J_0(k) - iJ_1(k)] = \frac{L_o}{2\pi\mu U} \cdot [1 - ike^{-ik}(Ci(k) + iSi(k) + i\frac{\pi}{2})] \quad (A-19)$$

The value of $L_o / 2\pi\mu UV_o$ from eq. A-19 is shown in Fig. A-2. In the figure, the exact Sears' value is also plotted. The agreement between them is fairly satisfactory in the reduced frequency region from 0 to 1.3. The value of reduced frequency 1.3 corresponds to the blade harmonic ($q=N$) in a propeller of area ratio about 0.4.

APPENDIX B.
GEOMETRICAL MEANING OF THE
SIMPLIFICATION IN THE KERNEL

The simplified expression of the kernel, eqs. 24, is obtained from the original kernel equation, eq. 22, by using two approximations, one in the integral path and the other in the direction of differentiation. The validity of these simplifications becomes clear when the geometrical significance of eq. 22 is compared with that of eqs. 24.

Equation 22 indicates the following manipulation: the inverse of the Descartes distance,

$$\frac{1}{R[(0, r, 0), (X, \rho, \theta)]} = \frac{1}{\sqrt{X^2 + r^2 + \rho^2 - 2r\rho \cos \theta}},$$

which has its ends on a group of helicoidal surfaces ($n = 1, 2, \dots, N$), is differentiated at both ends in the directions perpendicular to the surfaces and then integrated moving the end (X, ρ, θ) along the helical trajectory on the helicoidal surface $X = \frac{1}{a} \theta - \frac{1}{a} \bar{\theta}_n$.

On the other hand, the simplified eq. 24 implies a similar procedure, but, this time, the helicoidal surfaces are replaced by segments of planes. Since the greatest contribution of the integral in eq. 22 and eqs. 24 arises in the rather narrow region, where the helicoidal surface in eq. 22 can be regarded as a plane, eqs. 24 can be a very good approximation for eq. 22, because in this region the relative direction of the differentiation with respect to the vector $(0, r, 0) \rightarrow (X, \rho, \theta)$ is the same in both expressions. Numerical results have been obtained for K_2 when $r = .75$ and $\rho = .85$ and X is taken from $\frac{\theta_0}{2a}$ to $\frac{3\theta_0}{2a}$, derived from both expressions and from eq. 38 where the summation is replaced by integration. They are compared in the following:

K_2 for $q = 0, r = .75, \rho = .85$
 $a = 2\pi \quad a = \pi$

Eq. 22 from $X = \frac{\theta_0}{2a}$ to $\frac{3\theta_0}{2a}$	- 25.1	- 9.6
Eqs. 24, $m = 1$	- 24.7	- 9.0
Eq. 38 from $X = \frac{\theta_0}{2a}$ to $\frac{3\theta_0}{2a}$	- 23.8	- 10.8

The agreement among them is satisfactory for practical purposes.

The values of K_1 from eq. 22 and from eq. 25 derived from 24 are compared below for the same values of $r = .75$ and $\rho = .85$. (The half-angular chord $\theta_b = \phi_0 - \theta_0 = 10^\circ$ for the calculations.)

q	$K_1(\text{eq. 25})$	$K_1(\text{eq. 22})$		
		$a = 2\pi$	$a = \frac{3\pi}{2}$	$a = \pi$
0	228.0	218	214	205
1	224.3 - 5.71	216	- 61	
4	200.8 - 19.01	194	- 181	

APPENDIX C.
EVALUATION OF INTEGRAL

$$I_q = \int_{\psi_\ell}^{\psi_u} \frac{e^{i2q\psi}}{(\sqrt{1-k^2\sin^2\psi})^3} d\psi$$

Watkins¹⁰ derived the recurrence formula for the special integral limits $\psi_u = \frac{\pi}{2}$ and $\psi_\ell = 0$. A somewhat similar method gives the formula for general integral limits.

In the first place, the following notations are introduced:

$$\begin{aligned} I_{\nu,n}^e &= \int_{\psi_\ell}^{\psi_u} \frac{e^{i2n\psi}}{(1-k^2\sin^2\psi)^{\nu/2}} d\psi \\ &= I_{\nu,n}^c + i I_{\nu,n}^s \end{aligned} \quad (C-1)$$

$$= \int_{\psi_\ell}^{\psi_u} \frac{\cos 2n\psi}{(1-k^2\sin^2\psi)^{\nu/2}} d\psi + i \int_{\psi_\ell}^{\psi_u} \frac{\sin 2n\psi}{(1-k^2\sin^2\psi)^{\nu/2}} d\psi$$

The expression

$$\cos 2(n+1)\psi + \cos 2(n-1)\psi = \cos 2n\psi \left(2 - \frac{4}{k^2}\right) + \frac{4}{k^2} \cos 2n\psi (1-k^2\sin^2\psi), \quad (C-2)$$

gives the relation

$$I_{s,n+1}^c + I_{s,n-1}^c = 2\left(1 - \frac{2}{k^2}\right) I_{s,n}^c + \frac{4}{k^2} I_{1,n}^c \quad (C-3)$$

Also, if the relation

$$\int \frac{\sin\psi \cos\psi}{(1-k^2\sin^2\psi)^{3/2}} d\psi = \frac{1}{k^2} \frac{1}{(1-k^2\sin^2\psi)^{1/2}} \quad (C-4)$$

is used, the following expression is obtained:

$$I_{s,n+1}^c - I_{s,n-1}^c = -4 \left[\frac{1}{k^2} \frac{\sin 2n\psi}{(1-k^2 \sin^2 \psi)^{1/2}} \right] \begin{vmatrix} \psi_u \\ \psi_\ell \end{vmatrix} - \frac{2n}{k^2} I_{1,n}^c \quad (C-5)$$

Eliminating $I_{1,n}^c$ from eqs. C-3 and C-5,

$$(2n-1) I_{s,n+1}^c + (2n+1) I_{s,n-1}^c = 4n \left(1 - \frac{2}{k^2} \right) I_{s,n}^c + \frac{4}{k^2} \frac{\sin 2n\psi}{(1-k^2 \sin^2 \psi)^{1/2}} \begin{vmatrix} \psi_u \\ \psi_\ell \end{vmatrix} \quad (C-6)$$

In a similar way,

$$(2n-1) I_{s,n+1}^s + (2n+1) I_{s,n-1}^s = 4n \left(1 - \frac{2}{k^2} \right) I_{s,n}^s \quad (C-7)$$

$$- \frac{4}{k^2} \frac{\cos 2n\psi}{(1-k^2 \sin^2 \psi)^{1/2}} \begin{vmatrix} \psi_u \\ \psi_\ell \end{vmatrix}$$

Thus, considering

$$I_{s,q}^e = I_q \quad (C-8)$$

and using the relation of eq. C-1, the recurrence formula for I_q is written as

$$I_{q+1} = \frac{4q}{2q-1} \left(1 - \frac{2}{k^2} \right) I_q + \frac{2q+1}{2q-1} I_{q-1} - \frac{1}{2q-1} \frac{4}{k^2} \frac{e^{i2q\psi}}{(1-k^2 \sin^2 \psi)^{1/2}} \begin{vmatrix} \psi_u \\ \psi_\ell \end{vmatrix} \quad (C-9)$$

In order to use this formula, the evaluations of I_0 and I_1 are necessary. Some elementary calculations give

$$I_{s,0}^c = \frac{1}{1-k^2} \left[E(k, \psi) - k^2 \frac{(1/2) \sin 2\psi}{(1-k^2 \sin^2 \psi)^{1/2}} \right] \bigg|_{\psi_\ell}^{\psi_u},$$

$$I_{s,0}^s = 0,$$

$$I_{s,1}^c = \left(1 - \frac{2}{k^2}\right) I_{s,0}^c + \frac{2}{k^2} F(k, \psi) \bigg|_{\psi_\ell}^{\psi_u} \quad (C-10)$$

and

$$I_{s,1}^s = \frac{2}{k^2} \frac{1}{(1-k^2 \sin^2 \psi)^{1/2}} \bigg|_{\psi_\ell}^{\psi_u}$$

where $F(k, \psi)$ and $E(k, \psi)$ are the first and the second kind of incomplete elliptic integral. Combining the cosine and the sine terms,

$$I_0 = I_{s,0}^e = \frac{1}{1-k^2} \left[E(k, \psi) - k^2 \frac{(1/2) \sin 2\psi}{\sqrt{1-k^2 \sin^2 \psi}} \right] \bigg|_{\psi_\ell}^{\psi_u}, \quad (C-11)$$

$$I_1 = I_{s,1}^e = \left(1 - \frac{2}{k^2}\right) I_0 + \frac{2}{k^2} F(k, \psi) \bigg|_{\psi_\ell}^{\psi_u} + i \frac{2}{k^2} \frac{1}{(1-k^2 \sin^2 \psi)^{1/2}} \bigg|_{\psi_\ell}^{\psi_u} \quad (C-12)$$

APPENDIX D.
INTEGRATION J_1

The contribution of the small area including the singular point $\theta = \theta$, $\rho = r_p$ is

$$J_1 = \lim_{x \rightarrow 0} \int_{\rho=r_p-\epsilon_0}^{r_p+\epsilon_0} \int_{\theta=-\gamma}^{\gamma} - \frac{\partial^2}{\partial x^2} \frac{e^{-iq\theta}}{\sqrt{x^2+r^2+\rho^2-2r\rho \cos\theta}} d\theta d\rho \quad (D-1)$$

As is stated in "Evaluation of The Kernel (K_1)" on p. 10, the case of $|\gamma| \ll 1$, $\epsilon_0 \ll r_p$ is considered. Therefore

$$J_1 = \lim_{x \rightarrow 0} \int_{-\epsilon_0}^{\epsilon_0} \int_{-\gamma}^{+\gamma} - \frac{\partial^2}{\partial x^2} \frac{1}{\sqrt{x^2+\epsilon^2+r_p^2} \theta^2} d\epsilon d\theta \quad (D-2)$$

and taking the lim finally
 $x \rightarrow 0$

$$J_1 = - 4 \frac{1}{r_p} \sqrt{\frac{1}{(r_p \gamma)^2} + \frac{1}{(\epsilon_0)^2}} \quad (D-3)$$

Therefore,

$$\lim_{\epsilon_0 \rightarrow 0} J_1 = - 4 \frac{1}{r_p \epsilon_0} \quad (D-4)$$

APPENDIX E.
INTEGRATION J_3

The integration domain does not include the singular point, therefore J_3 can be evaluated by the recurrence relation obtained in Appendix C. However, the limiting process $\epsilon_0 \rightarrow 0$ precludes using a numerical method for the ρ integration. In this section this difficulty is overcome by evaluating the integral in an approximate but analytical form made possible because $\beta_1, \beta_2 \ll r_p$.

The limiting process is taken first, then in elliptic integral form,

$$J_3 = (-1)^{q+1} 2 \left[\int_{r_p - \beta_1}^{r_p - \epsilon_0} + \int_{r_p + \epsilon_0}^{r_p + \beta_2} \right] \frac{1}{(r_p + \rho)^3} \sum_{n=1}^N \int_{-\frac{1}{2}(\pi + \bar{\theta}_n - \bar{\theta}_b)}^{-\frac{1}{2}(\pi + \bar{\theta}_n + \frac{\bar{\theta}_0}{2})} \frac{e^{i2q\psi}}{\sqrt{1 - k^2 \sin^2 \psi}^3} d\psi d\rho$$

$$\text{where, } k^2 = \frac{4r_p \rho}{(r_p + \rho)^2} \quad (\text{E-1})$$

Further, J_3 is divided into two parts,

$$J_{31} = (-1)^{q+1} 2 \left[\int_{r_p - \beta_1}^{r_p - \epsilon_0} + \int_{r_p + \epsilon_0}^{r_p + \beta_2} \right] \frac{1}{(r_p + \rho)^3} \int_0^{-\pi} \frac{e^{i2q\psi}}{\sqrt{(1 - k^2 \sin^2 \psi)}^3} d\psi d\rho \quad (\text{E-2})$$

$$J_{32} = (-1)^{q+1} 2 \left[\int_{r_p - \beta_1}^{r_p - \epsilon_0} + \int_{r_p + \epsilon_0}^{r_p + \beta_2} \right] \frac{1}{(r_p + \rho)^3} \left[- \int_0^{-\frac{1}{2}(\pi - \bar{\theta}_b)} - \int_{-\frac{1}{2}(\pi + \frac{\bar{\theta}_0}{2})}^{-\pi} \right]$$

(eq. E-2 con't. on next page)

$$+ \sum_{n=2}^N \int_{-\frac{1}{2}(\pi + \bar{\theta}_n - \bar{\theta}_b)}^{-\frac{1}{2}(\pi + \bar{\theta}_n + \frac{\bar{\theta}_0}{2})} \left[\frac{e^{i2q\psi}}{\sqrt{1-k^2 \sin^2 \psi}} \right] d\psi d\rho \quad (E-3)$$

with $k^2 = \frac{4r_p \rho}{(r_p + \rho)^2}$ and

$$k' = \sqrt{1 - k^2}$$

J_{s1} can be written as

$$J_{s1} = J_{s1}^- + J_{s1}^+$$

$$\left. \begin{aligned} J_{s1}^- &= (-1)^{q+1} \frac{2}{(2r_p)^2} \int_{\frac{\epsilon_0}{2r_p - \epsilon_0}}^{\frac{\beta_1}{2r_p - \beta_1}} (1+k') I'_q dk' \\ J_{s1}^+ &= (-1)^{q+1} \frac{2}{(2r_p)^2} \int_{\frac{\epsilon_0}{2r_p + \epsilon_0}}^{\frac{\beta_2}{2r_p + \beta_2}} (1-k') I'_q dk' \end{aligned} \right\} \quad (E-4)$$

$$\text{where } I'_q = \int_0^{-\pi} \frac{e^{i2q\psi}}{\sqrt{1-k^2 \sin^2 \psi}} d\psi \quad (E-5)$$

The recurrence relations obtained in Appendix C can be adapted for the elliptic integral I'_q . Then

$$I'_{q+1} = - \left[\frac{4}{2q-1} \left(\frac{1+k'^2}{1-k'^2} \right) I'_q + \frac{2q+1}{2q-1} I'_{q-1} \right] \quad (E-6)$$

$$I'_0 = - \left[\frac{2}{k'^2} E \left(\sqrt{1-k'^2} \right) \right] \quad (E-7)$$

$$I'_1 = - \left[\frac{1+k'^2}{1-k'^2} I'_0 + \frac{4}{1-k'^2} K \left(\sqrt{1-k'^2} \right) \right] \quad (E-8)$$

where $K(k)$ and $E(k)$ are complete elliptic integrals of the first and second kind. These formulae give

$$\begin{aligned} I'_0 &= - \left[\frac{2}{k'^2} E \right] \\ I'_1 &= \left[Q \frac{2}{k'^2} E - \frac{4}{1-k'^2} K \right] \\ I'_2 &= - \left[(4Q^2-3) \frac{2}{k'^2} E - 4Q \frac{4}{1-k'^2} K \right] \\ I'_3 &= \left[\left(\frac{32}{3} Q^3 - \frac{29}{3} Q \right) \frac{2}{k'^2} E - \left(\frac{32}{3} Q^2 - \frac{5}{3} \right) \frac{4}{1-k'^2} K \right] \\ I'_4 &= - \left[\left(\frac{128}{5} Q^4 - \frac{144}{5} Q^2 + \frac{21}{5} \right) \frac{2}{k'^2} E - \left(\frac{128}{5} Q^3 - \frac{48}{5} Q \right) \frac{4}{1-k'^2} K \right] \end{aligned} \quad (E-9)$$

$$\text{where, } Q = \frac{1+k'^2}{1-k'^2}$$

In the following treatment, since $\beta_1, \beta_2 \ll r_p$ and hence $k' \ll 1$, the terms smaller than the zero power of k' in the integrand of eq. E-4 are neglected. The elliptic integral E and K can be expanded in powers of k'^2 as

$$\begin{aligned} E &= 1 + \frac{1}{2} \left(\ln \frac{4}{k'} - \frac{1}{2} \right) k'^2 + \frac{3}{16} \left(\ln \frac{4}{k'} - \frac{13}{12} \right) k'^4 + \dots \\ K &= \ln \frac{4}{k'} + \frac{1}{4} \left(\ln \frac{4}{k'} - 1 \right) k'^2 + \frac{9}{64} \left(\ln \frac{4}{k'} - \frac{7}{6} \right) k'^4 + \dots \end{aligned} \quad (E-10)$$

Hence, from eqs. E-9, a sufficient form of I'_q for the above-mentioned approximation is

$$I'_q \doteq (-1)^{q+1} 2 \left\{ [1 + (a - b \ln k') k'^2] \left(\frac{1}{k'^2} + A_q \right) - (c - \ln k') B_q \right\} \quad (E-11)$$

where

$$a = \frac{1}{2} (\ln 4 - \frac{1}{2})$$

$$b = \frac{1}{2}$$

$$c = \ln 4$$

and

	A_q	$B_q = 2q^2$
$q = 0$	0	0
1	2	2
2	16	8
3	134/3	18
4	448/5	32

Eq. E-4 becomes

$$J_{s1} \doteq \frac{1}{(r_p)^2} \int_{\frac{\epsilon_0}{2r_p - \epsilon_0}}^{\frac{\beta_1}{2r_p - \beta_1}} \left[\frac{1}{k'^2} + \ln k' (B_q - b) + (A_q + a - B_q c) + \frac{1}{k'} \right] dk'$$

$$\doteq \frac{1}{(r_p)^2} \left[-\frac{1}{k'} + k' (\ln k' - 1) (B_q - b) + k' (A_q + a - B_q c) + \ln k' \right] \bigg|_{\frac{\epsilon_0}{2r_p - \epsilon_0}}^{\frac{\beta_1}{2r_p - \beta_1}} \quad (E-12 \text{ Con't})$$

$$J_{s1}^+ \doteq \frac{1}{(r_p)^2} \left[-\frac{1}{k'} + k'(\ln k' - 1)(B_q - b) + k'(A_q + a - B_q c) - \ln k' \right] \left| \begin{array}{c} \beta_2 \\ 2r_p + \beta_2 \\ \epsilon_0 \\ 2r_p + \epsilon_0 \end{array} \right.$$

If β_1 and β_2 are chosen to satisfy the relation

$$\frac{\beta_1}{2r_p - \beta_1} = \frac{\beta_2}{2r_p + \beta_2} \quad (=k'_1) \quad , \quad (E-13)$$

$\lim_{\epsilon_0 \rightarrow 0} J_{s1}$ is given in the following form:

$$\begin{aligned} \lim_{\epsilon_0 \rightarrow 0} J_{s1} &= \lim_{\epsilon_0 \rightarrow 0} (J_{s1}^- + J_{s1}^+) \\ &= \frac{2}{(r_p)^2} \left[-\frac{1}{k'_1} + k'_1 (\ln k'_1 - 1) (B_q - b) \right. \\ &\quad \left. + k'_1 (A_q + a - B_q c) \right] \\ &\quad + \lim_{\epsilon_0 \rightarrow 0} \frac{4}{r_p \epsilon_0} \end{aligned} \quad (E-14)$$

As is seen in eq. E-3, even the point in the integration domain of J_{s2} which is closest to the singular point is at a distance from it equal to $r_p \bar{\theta}_b$, where $\bar{\theta}_b$ is the angular semi-chord.

If β_1 and β_2 are very small compared to $r_p \bar{\theta}_b$, k can be assumed unity throughout the whole integration domain of J_{s2} . Thus,

$$J_{32} \doteq \lim_{\epsilon_0 \rightarrow 0} (-1)^{q+1} 2 \left[2k'_1 - \frac{\epsilon_0}{r_p} \right] \frac{1}{(2r_p)^2}$$

$$\left[I''_q \left(- \begin{vmatrix} -\frac{1}{2}(\pi - \bar{\theta}_b) \\ 0 \end{vmatrix} - \begin{vmatrix} -\pi \\ -\frac{1}{2}(\pi + \frac{\bar{\theta}_0}{2}) \end{vmatrix} + \sum_{n=2}^N \begin{vmatrix} -\frac{1}{2}(\pi + \bar{\theta}_n + \frac{\bar{\theta}_0}{2}) \\ -\frac{1}{2}(\pi + \bar{\theta}_n - \bar{\theta}_b) \end{vmatrix} \right) \right] \quad (E-15)$$

where

$$I''_q \doteq \int \frac{e^{i2q\psi}}{\sqrt{1-\sin^2\psi}} d\psi \quad (E-16)$$

The recurrence relation obtained in Appendix C holds also for I''_q , but in this case it becomes

$$\begin{aligned} I''_{q+1} &= \frac{4q}{2q-1} (-1) I''_q - \frac{2q+1}{2q-1} I''_{q-1} - i(\pm) \frac{4}{2q-1} \frac{e^{i2q\psi}}{\cos\psi} \\ I''_0 &= \pm \left[\frac{\sin\psi}{2\cos^2\psi} + \frac{1}{2} \ln \left| \tan \left(\frac{\pi}{4} + \frac{\psi}{2} \right) \right| \right] \\ I''_1 &= (-1) I_0 + 2 F(k=1, \psi) + i2(\pm) \frac{1}{\cos\psi} \\ (I''_1) &= \mp \frac{\sin\psi}{2\cos^2\psi} \pm \frac{3}{2} \ln \left| \tan \left(\frac{\pi}{4} + \frac{\psi}{2} \right) \right| \pm i2 \frac{1}{\cos\psi}, \end{aligned} \quad (E-17)$$

where the double sign should be taken in the following sense:

- + for the region $\cos\psi > 0$
- for the region $\cos\psi < 0$

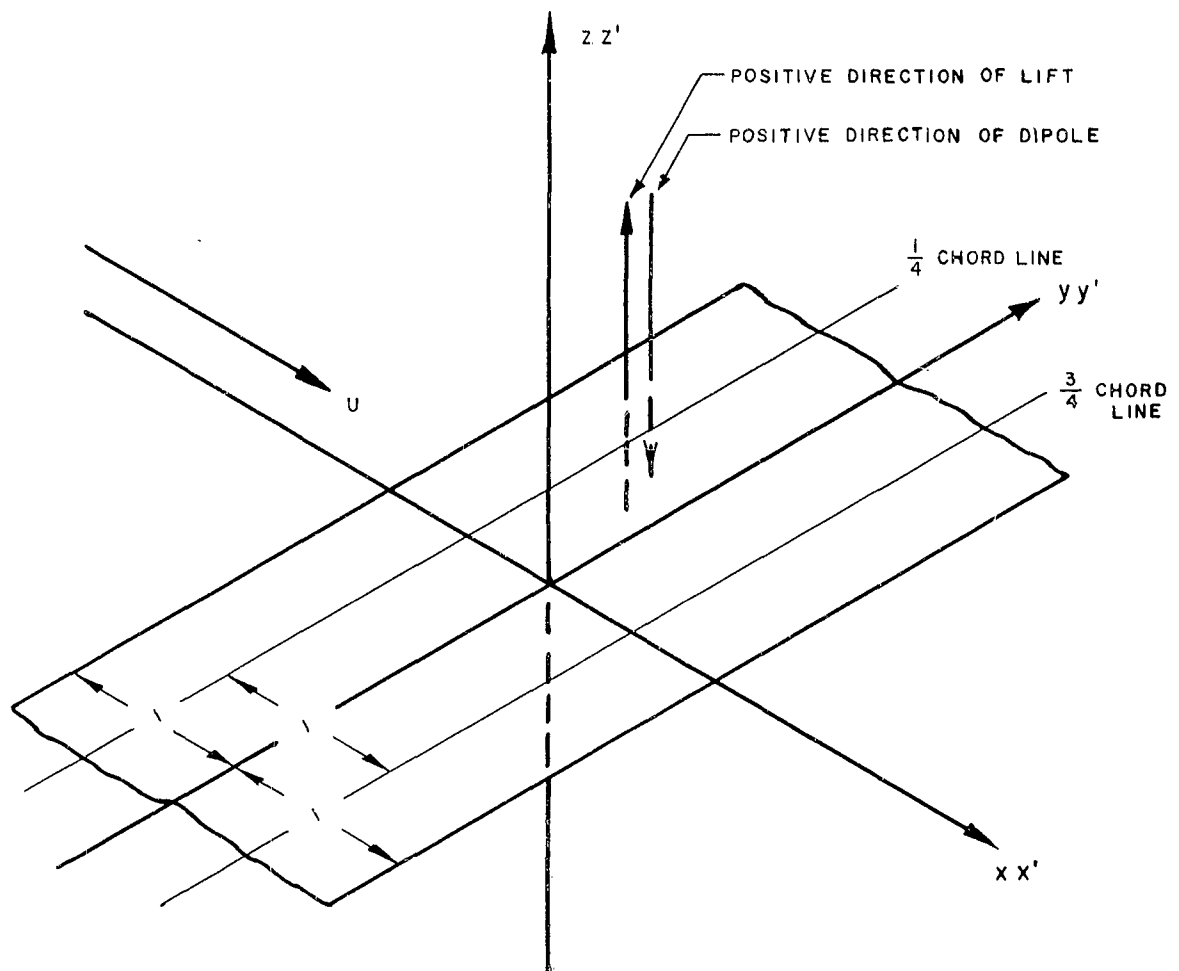


FIGURE A-1. COORDINATE SYSTEM AND NOTATIONS FOR TWO-DIMENSIONAL WEISSINGER MODEL

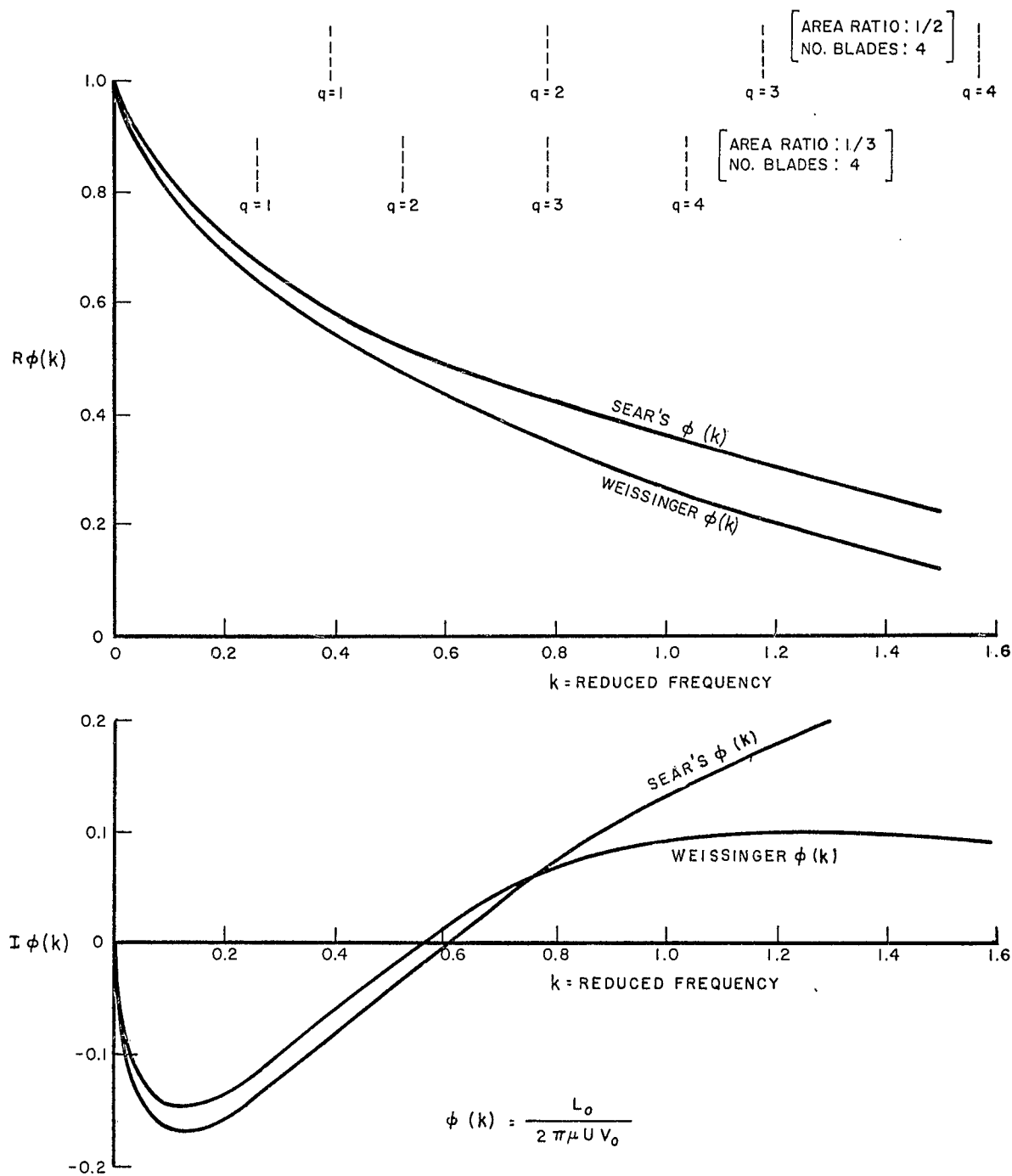


FIGURE A-2. APPLICATION OF WEISSINGER METHOD TO SEAR'S GUST PROBLEM FOR NON-STATIONARY CASE

R-940

DISTRIBUTION LIST

Copies

Copies

60	Commanding Officer and Director David Taylor Model Basin Washington 7, D.C. Attn: Code 513	Capt. E. S. Arentzen, USN Commanding Officer U. S. Naval Reserve Offices Training Corps Massachusetts Institute of Technology Cambridge 39, Massachusetts	1
9	Chief, Bureau of Ships Department of the Navy Washington 25, D.C. Attn: Tech. Library (210L)(3) Ship Design (Code 410)(1) Ship Silencing Br (345)(1) Prelim. Design (420)(2) Hull Design (Code 440)(1) Scientific and Research (Code 442)(1)	Dr. J. V. Wehausen Department of Engineering Institute of Engineering Research University of California Berkeley 4, California	1
2	Director Ordnance Research Laboratory Pennsylvania State University P. O. Box 30 University Park, Pennsylvania	Librarian Society of Naval Architects and Marine Engineers 74 Trinity Place New York, New York	1
1	Mr. Hollinshead De Luce Bethlehem Steel Company Shipbuilding Division Central Technical Division Quincy 69, Massachusetts	Professor R. B. Couch Chairman Department of Naval Architecture and Marine Engineering University of Michigan Ann Arbor, Michigan	2
2	Gibbs and Cox, Inc. 21 West Street New York 6, N. Y. Attn: Mr. W. F. Gibbs Mr. W. Bachman	Propulsion Division (P8063) U. S. Naval Ordnance Test Station 125 S. Grand Avenue Pasadena, California	1
1	Reed Research Inc. 1048 Potomac Street, N.W. Washington 7, D.C. Attention: Mr. S. Reed	Administrator Webb Institute of Naval Architecture Glen Cove, New York Attn: Post Graduate School for Officers	2
1	Dr. A. G. Strandhagen, Head Dept. of Engineering Mechanics University of Notre Dame Notre Dame, Indiana	Mr. John Kane Engineering Technical Department Newport News Shipbuilding and Dry Dock Company Newport News, Virginia	1
2	Dept. of Naval Architecture and Marine Engineering Massachusetts Inst. of Technology Cambridge 39, Massachusetts		

DISTRIBUTION LIST

Copies			Copies
1	Mr. V. L. Russo, Deputy Chief Officer of Ship Construction Maritime Administration Washington 25, D. C.	Commanding Officer Office of Naval Research Branch Office Navy 100, F. P. O. New York, New York	15
1	Mr. Caesar Tangerini, Head Main Propulsion Section Engineering Specification Branch Maritime Administration Washington 25, D. C.	Dr. L. G. Straub, Director St. Anthony Falls Laboratory University of Minnesota Minneapolis, Minnesota	1
1	Editor Applied Mechanics Review Southwest Research Institute 8500 Culebra Road San Antonio 6, Texas	Commander Defense Documentation Center Attention: TIPDR Arlington Hall Station Arlington 12, Virginia	10
5	Chief of Naval Research Department of the Navy Washington 25, D. C. For distribution to: Code 438 (4) Code 466 (1)	Chief, Bureau of Naval Weapons Department of the Navy Washington 25, D. C.	1
1	Director U. S. Naval Research Laboratory Code 2000 Washington 25, D. C.	Commander U. S. Naval Ordnance Laboratory White Oak - Silver Spring, Md. Attention: Library	2
3	Commander U. S. Naval Ordnance Test Station Pasadena Annex 3202 East Foothill Boulevard Pasadena, California For additional distribution to: Technical Library (1) Head, Thrust Producer Sec. (1)	Commanding Officer Office of Naval Research 495 Sumner Street Boston 10, Massachusetts	1
1	Commanding Officer Office of Naval Research Branch Office 207 W. 24th Street New York 11, New York	Commanding Officer Office of Naval Research The John Crerar Library Building 86 E. Randolph Street - 10th floor Chicago 1, Illinois	1
1	Commanding Officer Office of Naval Research Branch Office 1000 Geary Street San Francisco 9, California	Commanding Officer Office of Naval Research 1030 East Green Street Pasadena 1, California	1
		Director, Hydrodynamics Lab. California Institute of Technology Pasadena 4, California	1

DISTRIBUTION LIST

Copies

- 1 Professor J. A. Schade, Director
Institute of Engineering Research
University of California
Berkeley 4, California
- 1 Editor, Engineering Index, Inc.
29 West 39th Street
New York, New York
- 1 Librarian, Institute of Aerospace
Sciences, Inc.
2 East 64th Street
New York 21, New York
- 1 Dr. Jack Kotik
Technical Research Group
2 Aerial Way
Syosset, L.I., N.Y.

Davidson Laboratory Report No. 940
THREE-DIMENSIONAL APPROACH TO THE
GUST PROBLEM FOR A SCREW PROPELLER

by J. Shioiri and S. Tsakonas

UNCLASSIFIED

The unsteady lifting surface approach is utilized for the marine propeller case and the corresponding surface integral equation is solved for the Weissinger mathematical model. The applicability of the Weissinger method to the nonstationary flow case is studied. The kernel function is expressed in closed forms after some mathematical simplification. From numerical calculations of propeller loading which are restricted to a four-bladed propeller of sector type blade form with different blade-area ratios and various pitch-diameter ratios, conclusions are drawn as to three-dimensional effects as well as to the dependence of propeller loading on the important parameters, as the blade-area and pitch-diameter ratios.

Davidson Laboratory Report No. 940
THREE-DIMENSIONAL APPROACH TO THE
GUST PROBLEM FOR A SCREW PROPELLER

by J. Shioiri and S. Tsakonas

UNCLASSIFIED

The unsteady lifting surface approach is utilized for the marine propeller case and the corresponding surface integral equation is solved for the Weissinger mathematical model. The applicability of the Weissinger method to the nonstationary flow case is studied. The kernel function is expressed in closed forms after some mathematical simplification. From numerical calculations of propeller loading which are restricted to a four-bladed propeller of sector type blade form with different blade-area ratios and various pitch-diameter ratios, conclusions are drawn as to three-dimensional effects as well as to the dependence of propeller loading on the important parameters, as the blade-area and pitch-diameter ratios.

Davidson Laboratory Report No. 940
THREE-DIMENSIONAL APPROACH TO THE
GUST PROBLEM FOR A SCREW PROPELLER

by J. Shioiri and S. Tsakonas

UNCLASSIFIED

The unsteady lifting surface approach is utilized for the marine propeller case and the corresponding surface integral equation is solved for the Weissinger mathematical model. The applicability of the Weissinger method to the nonstationary flow case is studied. The kernel function is expressed in closed forms after some mathematical simplification. From numerical calculations of propeller loading which are restricted to a four-bladed propeller of sector type blade form with different blade-area ratios and various pitch-diameter ratios, conclusions are drawn as to three-dimensional effects as well as to the dependence of propeller loading on the important parameters, as the blade-area and pitch-diameter ratios.

Davidson Laboratory Report No. 940
THREE-DIMENSIONAL APPROACH TO THE
GUST PROBLEM FOR A SCREW PROPELLER

by J. Shioiri and S. Tsakonas

UNCLASSIFIED

The unsteady lifting surface approach is utilized for the marine propeller case and the corresponding surface integral equation is solved for the Weissinger mathematical model. The applicability of the Weissinger method to the nonstationary flow case is studied. The kernel function is expressed in closed forms after some mathematical simplification. From numerical calculations of propeller loading which are restricted to a four-bladed propeller of sector type blade form with different blade-area ratios and various pitch-diameter ratios, conclusions are drawn as to three-dimensional effects as well as to the dependence of propeller loading on the important parameters, as the blade-area and pitch-diameter ratios.